NUCLEAR ENERGY RESEARCH INITIATIVE (NERI)

FINAL REPORT
July 2007– December 2010

An Advanced Integrated Diffusion/Transport Method for the Design, Analysis and Optimization of the Very-High-Temperature Reactors

DE-FC07-07ID14821

Submitted by:

Lead Organization: Georgia Institute of Technology

PI: Farzad Rahnema
Co-PI: Dingkang Zhang

Collaborating Organization(s): Idaho National Laboratory
Co-PI: Abderrafi Ougouag
Frederick Gleicher

SUMMARY

The main objective of this research is to develop an integrated diffusion/transport (IDT) method to substantially improve the accuracy of nodal diffusion methods for the design and analysis of Very High Temperature Reactors (VHTR). Because of the presence of control rods in the reflector regions in the Pebble Bed Reactor (PBR-VHTR), traditional nodal diffusion methods do not accurately model these regions, within which diffusion theory breaks down in the vicinity of high neutron absorption and steep flux gradients. The IDT method uses a local transport solver based on a new incident flux response expansion method in the controlled nodes. Diffusion theory is used in the rest of the core. This approach improves the accuracy of the core solution by generating transport solutions of controlled nodes while maintaining computational efficiency by using diffusion solutions in nodes where such a treatment is sufficient. The transport method is initially developed and coupled to the reformulated 3-D nodal diffusion model in the CYNOD code for PBR core design and fuel cycle analysis.

This method is also extended to the prismatic VHTR. The new method accurately captures transport effects in highly heterogeneous regions with steep flux gradients. The calculations of these nodes with transport theory avoid errors associated with spatial homogenization commonly used in diffusion methods in reactor core simulators.

I. INTRODUCTION

The current generation of core neutronics methods is based on nodal diffusion theory and utilizes homogenized cross sections and other physics data generated by single assembly, infinite medium transport theory calculations. This reactor analysis methodology was developed and refined for the currently operating class (Generation II) of light water reactors (LWRs). Until about a decade ago, the reload cores of these reactors were designed with relatively homogeneous distributions of fuel, moderator, and absorber materials. For these systems, core-level diffusion theory is a good approximation, and the computational de-coupling of fuel assemblies for generating physics data is acceptable.

The current trend in reactor cores, however, is toward higher degrees of heterogeneity. In order to lengthen operating cycles, recent cores have been designed with higher amounts of total fissile mass which has necessitated the addition of burnable absorbers to hold down the reactivity at the beginning of core life. Increased fuel utilization has been achieved by varying the fuel enrichment within assemblies and optimizing the arrangement of assemblies with significantly different fissile and fission product compositions.

The extension of this approach to Very-High-Temperature Reactors (VHTRs) seems inadequate for a number of reasons. Firstly, VHTRs may be highly heterogeneous reactors (e.g. the double heterogeneity of pebble bed reactors), and the ad-hoc measures to account for double heterogeneity in LWRs (such as Dancoff correction factors for resonance absorption) are not adequate for the third spatial dimension. In LWRs, the axial nuclide densities are sufficiently slowly varying such for this approximation to be workable. In the PBR-VHTR, however, the fuel-moderator distribution is doubly heterogeneous in all three dimensions and must be modeled accordingly. The extent to which the 3D pebble-grain distributions affect the Dancoff correction factor (and hence, resonance absorption) is currently an active area of research for the PBR-VHTR. Secondly, the inaccuracy in the determination of reflector cross sections is of major concern for these types of reactors, especially since several designs confine the control rods to the reflector regions. Thirdly, it is well known that diffusion theory is not valid near strong absorbers (control rods) and interfaces with large material discontinuities including the external boundary of the system. As a consequence, standard nodal methods based on infinite-medium homogenized cross sections cannot be expected to provide detailed spatial flux reconstruction, estimations of peak pin power and estimates of control rod worth with the level of accuracy that is needed for reactor safety analysis.

A suitable methodology for the VHTR (both PBR and prismatic) should be able to treat nodes with high heterogeneity including reflector regions containing control rods, for the strong transport effects expected therein. In addition, the computational cost of the proposed methodology should be of primary importance for reactor simulations; thus it must retain both the speed and scalability to 3-D problems presented by nodal methods.

This final report is divided into five major sections. Section II contains an overview summarizing the objectives, work scope, and products of the project. In Section III is a list of the publications generated by this project. In Section IV contains a complete description of the work performed in this project. Finally, Section V highlights the project accomplishments.

II. PROJECT OVERVIEW

Objective

The main objective of the proposed project is to develop a novel methodology to substantially improve the accuracy of current nodal diffusion methods for the design and analysis of new Very-High-Temperature Reactor (VHTR) designs. The method is to be implemented in existing diffusion codes. It was expect that the new approach will achieve a significantly higher degree of accuracy than current industry (diffusion) methods, especially for heterogeneous reactors.

Work Scope

The main scope of work involves the development of an integrated diffusion/transport (IDT) method, the implementation of the method in existing diffusion codes, the development of PBR and prismatic VHTR benchmark problems, and the evaluation of the implemented method. The first year effort was focused on 2-D (r, z) cylindrical geometry applications. In year 2, the IDT method was extended to 2-D (r, theta) cylindrical geometry. In the third year, the IDT method was extended and fully tested in 3-D cylindrical geometry. In addition, the IDT method in 2-D hexagonal geometry was developed and implemented into the diffusion code PARCS.

The project was a collaborative effort of three organizations: Georgia Institute of Technology and Idaho National Laboratory (INL). As the lead organization, Georgia Tech's responsibility was to develop and implement the transport method for LWR calculations. The INL provided expertise in the area of PBR calculations, and was responsible for incorporating the coarse-mesh computational module(s) into the diffusion code CYNOD.

Products

The products developed as a result of this project are listed below:

1. An integrated nodal transport/diffusion code for whole core calculations in the 3-D cylindrical geometry for the pebble bed design option of the VHTR. This method, which is implemented into CYNOD, has the accuracy close to that of pure transport methods because of its capability to treat highly absorbing nodes (such as controlled reflector nodes) by a local transport solver.

2. A new 2-D response function transport method in hexagonal geometry for the prismatic design option of the VHTR. Improved accuracy is achieved when this new transport method is implemented into PARCS.

3. New benchmark problems for both VHTR options.

4. A series of publications and reports documenting the results of the project

III. PUBLICATIONS

This section lists the publications that resulted from this project. These papers are referenced throughout this report by citing the reference number between brackets, […]. Other references appear as footnotes at the bottom of the page where they are cited.

1. D. Zhang, and F. Rahnema, "Local Transport Method for Hybrid Diffusion/Transport Calculations in 2-D Cylindrical (R,Theta) Geometry," International Conference on Mathematics and Computational Methods Applied to Nuclear Science and Engineering (M&C 2011) Rio de Janeiro, RJ, Brazil, May 8-12, 2011 (accepted).

2. Zhan Zhang, Farzad Rahnema, Dingkang Zhang, Justin Pounders, Abderrafi Ougouag, "Simplified two and three dimensional HTTR benchmark problems," Annals of Nuclear Energy, vol. 38 (2011), pp. 1172–1185

3. R. Hayward, F. Rahnema, and D. Zhang, "An Integrated Diffusion-Transport Solution for a Simplified HTR Problem," Transactions of the American Nuclear Society (2011) (accepted).

4. R. Hayward, F. Rahnema, and D. Zhang, "An Integrated Diffusion-Transport method for Hexagonal Geometry: A Proof-of-Concept Study," International Conference on Mathematics and Computational Methods Applied to Nuclear Science and Engineering (M&C 2011) Rio de Janeiro, RJ, Brazil, May 8-12, 2011 (accepted).

5. D. Zhang and F. Rahnema, "Coarse Mesh Transport Method for Whole Core Neutronics Analysis in Cylindrical Geometry," 17th Pacific Basin Nuclear Conference, Cancun. W.R., Mexico, October 24-30, 2010.

6. D. Zhang, F. Rahnema, A. M. Ougouag and F. Gleicher, "Local Response-Function-Based Transport Method for Diffusion-Transport Hybrid Calculations in Pebble Bed Reactors," 5th International Conference on High Temperature Reactor Technology (HTR 2010), Prague, Czech Republic, October 18-20, 2010.

7. D. Zhang, F. Rahnema, A. Ougouag, "New Expansion Functions for Calculation of Coarse Mesh Response Functions", ANS 2007 Annual Meeting, Boston, MA, June 24-28, 2007.

IV. MAJOR TASKS

A. Task 1.1: Develop 2D(*r*, θ) response function-based transport method, *Georgia Tech*

1. Task Status and Significant Results

a. Task Summary

This aim of this task is to develop a 2-D cylindrical transport method to generate response functions, in terms of exiting partial currents, surface-averaged and node-averaged scalar fluxes, for non-multiplying regions such as inner and outer reflectors to couple with the diffusion method. This task is essentially to develop a set of expansion functions, which is suitable for coupling with 2-D cylindrical diffusion methods on the interfaces between diffusion and transport regions, to expand/approximate particle phase space distributions. These expansion functions will be used as boundary conditions to generate local solutions (i.e. response functions) for each unique coarse mesh in Task 1.3.

b. Task Status/Progress

b1. Conventional Legendre Polynomial Expansion

To generate response functions for a coarse mesh, an approximation of neutron phase space distributions on the mesh boundaries must be made since the whole core solution is not known a priori. Conventionally, it is assumed that the interface angular current $j\left(\vec{r},\hat{\Omega},E\right)$ can be expanded in terms of multi-products of Legendre polynomials as shown in Eq. (A.1), and then response functions are calculated by solving each local fixed source problem with an incoming flux imposed on the mesh boundaries.

$$j^{\pm}\left(\vec{r},\mu,\varphi,E\right)=\sum_{lmnp}J^{\pm}_{lmnp}P_l\left(\vec{r}\right)P_m\left(\mu\right)P_n\left(\varphi\right)P_p\left(E\right) \tag{A.1}$$

or equivalently,

$$\psi^{\pm}\left(\vec{r},\mu,\varphi,E\right)=\frac{1}{\left(\vec{n}^{\pm}\cdot\hat{\Omega}\right)}\sum_{lmnp}J^{\pm}_{lmnp}P_l\left(\vec{r}\right)P_m\left(\mu\right)P_n\left(\varphi\right)P_p\left(E\right) \tag{A.2}$$

In above equations, $\vec{r}$ represents spatial variable on the mesh interface, $\hat{\Omega}$ is the neutron direction, φ and μ denote the azimuthal and polar angle variables, respectively, *E* represents neutron energy, $\vec{n}^{\pm}$ is the outward or inward normal to the mesh interface at point $\vec{r}$, $P_n(x)$ is the n-th order scaled Legendre polynomial, and $J^{\pm}_{lmnp}$ represents expansion coefficients or partial current moments.

Obviously, the 0^{th} order expansion function represents a spatially uniform and angularly isotropic surface source with a flat energy spectrum. Accordingly, the 0^{th} expansion moment is identical to the total partial current. Because of the orthogonalities of Legendre polynomials, a higher order expansion only changes the shape of the neutron distribution functions, while the total partial current still remains unchanged.

Though this expansion can guarantee that intra-nodal partial currents are conserved, it introduces singularities in scalar fluxes and consequently cannot be used by transport methods that couple to diffusion methods, in which response functions, in terms of surface-averaged fluxes, are required. In thermal reactors, the angular flux in most regions is dominated by its isotropic component; it would be physically natural to require the 0^{th} order angular expansion function to be equivalent to the isotropic angular flux.

b2. Requirements of New Expansion Functions in 2D Cylindrical Geometry

Based on the discussion above, the following are the desirable characteristics of a new set of expansion functions:

1) The scalar flux resulting from the expansion is finite;
2) total partial currents remain unchanged after an expansion;
3) the 0^{th} angular expansion function is constant in angle (isotropic).

To avoid singularities introduced by an expansion, angular fluxes instead of angular currents should be chosen to be expanded in both the outward and inward hemispheres as in the following form.

$$\psi^{\pm}\left(\vec{r},\hat{\Omega},E\right)=\sum_{i,j,k,l} c^{\pm}_{ijkl}\, f_{ijkl}\left(\vec{r},\hat{\Omega},E\right) \tag{A.3}$$

where $c^{\pm}_{ijkl}$ are expansion coefficients, f_{ijkl} represent expansion functions which satisfy the following orthogonality condition.

$$\begin{aligned}&\int_S d\vec{r}\int dE \int_{\left(\vec{n}^{\pm}\cdot\hat{\Omega}>0\right)} d\hat{\Omega}\left(\vec{n}^{\pm}\cdot\hat{\Omega}\right) f_{ijkl}\left(\vec{r},\hat{\Omega},E\right) f_{i'j'k'l'}\left(\vec{r},\hat{\Omega},E\right)\\ &= A_{ijkl}\delta_{ii'}\delta_{jj'}\delta_{kk'}\delta_{ll'}\end{aligned} \tag{A.4}$$

where *S* represents the mesh interface, δ is the Kronecker delta, A_{ijkl} are constants, and the factor $\vec{n}^{\pm}\cdot\hat{\Omega}$ is a weighting function. By using the above condition, the expansion coefficients $c^{\pm}_{ijkl}$ can be defined by the following relation with the angular flux $\psi^{\pm}\left(\vec{r},\hat{\Omega},E\right)$.

$$c^{\pm}_{ijkl}=\int_S d\vec{r}\int dE \int_{\vec{n}^{\pm}\cdot\hat{\Omega}>0} d\hat{\Omega}\left(\vec{n}^{\pm}\cdot\hat{\Omega}\right) f_{ijkl}\left(\vec{r},\hat{\Omega},E\right)\psi^{\pm}\left(\vec{r},\hat{\Omega},E\right) \tag{A.5}$$

It should be pointed out that the commonly used spherical harmonic functions are defined in the whole 4π solid angle and does not satisfy the orthogonality condition (A.4), and consequently cannot be used as the expansion functions in this research.

b3. New Expansion Functions in 2D Cylindrical Geometry

For a 2D cylindrical surface shown in Figure 1 in which axis *z* is chose to be parallel with the axis of the cylinder and *y* is along the outward/inward normal direction at point $\vec{r}$, new

expansion functions are a tensor product of Legendre polynomials $P_n(x)$ and Chebyshev polynomials of the second kind $U_n(x)$:

$$f_{ijkl}(\vec{r},\hat{\Omega},E) = P_i(\vec{r})U_j(\cos\theta)P_k(\cos\varphi)P_l(E) \tag{A.6}$$

where *i*, *j*, *k* and *l* are expansion orders in spatial, polar angle, azimuthal angle and energy variables, respectively. Chebyshev polynomials $U_n(\mu)$ have the recurrence relation given below.

$$\begin{aligned} &U_0(\mu) = 1 \\ &U_1(\mu) = 2\mu \\ &U_{n+1}(\mu) = 2\mu U_n(\mu) - U_{n-1}(\mu) \quad \text{for } n \geq 1 \end{aligned} \tag{A.7}$$

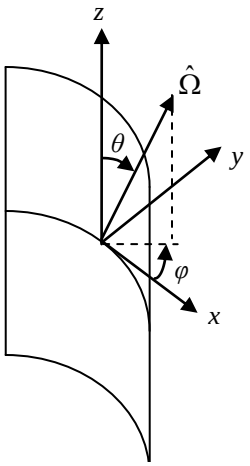

Fig. A1: Angular variables in a 2D cylindrical surface

Apparently, the 0th order expansion is a constant and consequently represents a flux which is isotropically distributed over the outward hemisphere and uniformly distributed over the 2D cylindrical surface. From equation (A.6), we can calculate the 0th expansion coefficient as

$$c^{\pm}_{0000} = \int_S ds \int dE \int_{\vec{n}^{\pm}\cdot\hat{\Omega}>0} d\hat{\Omega}\left(\vec{n}^{\pm}\cdot\hat{\Omega}\right)\psi^{\pm}(\vec{r},\hat{\Omega},E) \tag{A.8}$$

It is evident that the 0th expansion moment is identical to the total partial incoming/outgoing current crossing the mesh boundary when the new 2D expansion functions are used. As a result, the total partial currents (or particles) based on these expansions are always conserved. The new expansion functions also avoid the singularity introduced by the conventional Legendre polynomial expansion since the lowest order expansion function represents an isotropic flux. These new expansion functions will be used as a boundary condition imposed on an inner/outer coarse mesh to generate response functions for coupling with the diffusion solutions in fuel regions.

b4. Local transport method in 2D Cylindrical Geometry

The coarse-mesh methodology for the transport treatment of a set of selected nodes has been tailored to match the requirements of the CMFD method. The response functions of the coarse mesh corresponding to an incoming current from one of the adjacent regions can be calculated by solving the local problem below.

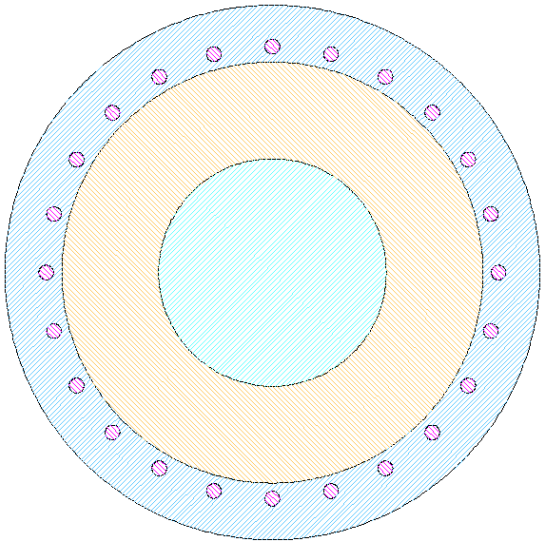

Fig. A2: 2-D simplified PBMR400 model

$$\frac{\mu}{r}\frac{\partial}{\partial r}\left(r\psi_i\left(r,\theta,\hat{\Omega},E\right)\right)+\frac{\eta}{r}\frac{\partial}{\partial\theta}\psi_i\left(r,\theta,\hat{\Omega},E\right)-\frac{1}{r}\frac{\partial}{\partial\omega}\left(\eta\psi_i\left(r,\theta,\hat{\Omega},E\right)\right)$$
$$+\sigma_t\left(r,\theta,E\right)\psi_i\left(r,\theta,\hat{\Omega},E\right)=Q_i\left(r,\theta,\hat{\Omega},E\right)+\int_0^\infty dE'\int_{4\pi}d\Omega'\ \sigma_s\left(r,\theta,\hat{\Omega}',E'\to\hat{\Omega},E\right)\psi_i\left(r,\theta,\hat{\Omega}',E'\right) \quad \text{(A.9)}$$

with the following boundary condition

$$\psi_i^-\left(r_{ij},\theta_{ij},\hat{\Omega},E\right)=\psi_j^+\left(r_{ij},\theta_{ij},\hat{\Omega},E\right) \quad \text{(A.10)}$$

where $(r_{ij},\theta_{ij})\in\left\{V_i\cap V_j\right\}$ for all V_j bounding V_i.

In the above equations, $\psi_i\left(r,\theta,\hat{\Omega},E\right)$ is the neutron angular flux within coarse mesh *i*, r and θ are spatial variables in the cylindrical coordinate, ω and ξ are angular variables. Q is the internal volumetric source that may also include scattering neutrons. V_i represents all the sub-volume elements (i.e. coarse meshes). The superscripts "+" and "-"on the angular flux indicate the outgoing and incoming direction, respectively.

B. Task 1.2: Develop 2D(*r, θ*) RMNB diffusion method, *INL*

1. Task Status and Significant Results

Introduction

The goal of this work is to include transport treatment in selected nodes of a diffusion nodal code. The targeted nodes are non-multiplying regions in the reflector of a pebble bed reactor

with control rods or voids in the locations of the control rods. Transport effects are captured through the use of response functions. The response functions can be manipulated in such a way that they form a set of equations that can be easily incorporated into the nodal diffusion code.

CMFD Derivation from Nodal Green's Function Approach

The derivation of the nodal Green's function method is well known and can be found in many sources. Expressions for the edge currents are obtained in terms of Green's functions, average scalar fluxes, and nodal source terms. These expressions are then used to obtain a banded system of equations for the nodal scalar flux in the Direct Coarse Mesh Finite Difference (Direct CMFD) form. The system of equations is iterated upon until the scalar flux converges to a specified tolerance.

Algorithm of the CYNOD Code for Analysis of PBRs

The banded systems of equations that result from the derivation with the Green's function for the scalar flux have been implemented in the CYNOD code. The CYNOD code solves for the scalar flux with a direct tri-diagonal solver when the radial, axial and angular cylindrical directions are obtained separately. When the directions are coupled, the angular flux is obtained by iterating on the banded matrix.

The generation of the coefficients of the matrix coupling the fluxes within the neutronic solver inside CYNOD can be obtained from diffusion theory, as described above of from transport theory when the corresponding response functions are available. The response function treatment within the CYNOD solver is discussed next.

Derivation of the Response Function Treatment for CYNOD

The outward current, average nodal scalar flux and edge scalar flux values are formulated in terms of response functions and the edge currents are expressed in terms of the outward and inward facing currents. The edge current equations and the outward current response function formulation are algebraically manipulated to obtain expressions for the nodal inward facing currents. These nodal inward facing current relations are then substituted into the response function formulation of the average scalar flux to obtain the nodal response balance equation. Next the response function formulated edge scalar flux values are set equal to the edge scalar flux values of a designated transport nodes or they are set equal to the edge scalar flux values multiplied by a discontinuity factor of designated diffusion nodes. This results in a continuous flux interface equation that has currents as the unknowns. The inward currents obtained from the nodal balance equation are substituted into the flux interface expression. For an interface between a transport node and a diffusion-node edge currents obtained from the balance equation are substituted into flux interface expression.

When applied, the process described above and in the previous section results in the derivation of equations that relate the nodal scalar fluxes in three consecutive nodes. The collection of these equations yields a system of linear equations that can be cast into matrix form. The system contains coefficients that are obtained either from diffusion theory or from transport theory depending on the type of node considered. The unknowns are the nodal scalar fluxes over the extent of the reactor.

C. Task 1.3: Develop 2D(r, θ) response function-based transport method and RMNB method into the code, *Georgia Tech/INL*

1. Task Status and Significant Results

a. Task Summary

The aim of this task is to implement the 2D(r, θ) response function-based transport method developed in task 1.1 and RMNB diffusion method developed in task 1.2 into the code for hybrid diffusion/transport calculations of neutron transport in Pebble Bed Reactors (PBRs). This task consists of the following two subtasks: 1) implementation of the 2D(r, θ) response function-based transport method into the MCNP code to generate response functions for inner and outer reflectors; and 2) implement the 2D(r, θ) RMNB diffusion method into the CYNOD code.

b. Task Status/Progress

b1. HYBRID DIFFUSION/TRANSPORT METHOD

Suppose that the spatial domain of interest V can be divided into two domains: the transport domain V_T in which the transport effects are very import and the diffusion domain V_D in which the traditional diffusion theory is valid. The neutron flux distribution within region V_D can be computed by solving the following transport problem.

$$\begin{aligned}
&\mathbf{H}\psi_T\left(\vec{r},\hat{\Omega},E\right)=\frac{1}{k}\mathbf{F}\psi_T\left(\vec{r},\hat{\Omega},E\right) \qquad \vec{r}\in V_T \\
&\psi_T\left(\vec{r},\hat{\Omega},E\right)=\frac{\phi_D\left(\vec{r},E\right)+3\hat{\Omega}\cdot\vec{j}_D\left(\vec{r},E\right)}{4\pi} \qquad \vec{r}\in\partial V_{DT},\ \ \hat{n}_T\cdot\hat{\Omega}<0 \\
&\psi_T\left(\vec{r},\hat{\Omega},E\right)=\mathbf{B}\psi_T\left(\vec{r}',\hat{\Omega}',E'\right) \qquad \vec{r},\vec{r}'\in\partial V,\ \ \hat{n}\cdot\hat{\Omega}<0 \text{ and } \hat{n}\cdot\hat{\Omega}'>0
\end{aligned} \tag{C1}$$

where $\psi_T\left(\vec{r},\hat{\Omega},E\right)$ is the angular flux in the transport region, **H** and **F** represent the usual transport operators, ∂V is the external boundary of the entire spatial domain V, k is the eigenvalue of the global system, ∂V_{DT} denotes the interface between the diffusion and transport regions, $\hat{n}$ and $\hat{n}_T$ stand for the outward normal at the external boundary ∂V and interface ∂V_{DT}, respectively. **B** is the boundary operator (such as vacuum, specular and albedo boundary conditions) on ∂V. $\phi_D\left(\vec{r},E\right)$ is the scalar flux within the diffusion domain, which is computed by the diffusion method, and the net current $\vec{j}_D\left(\vec{r},E\right)$ is defined as:

$$\vec{j}_D\left(\vec{r},E\right)=-D\left(\vec{r},E\right)\nabla\phi_D\left(\vec{r},E\right) \tag{C2}$$

where D is the diffusion coefficient.

It is should be pointed out that Equation (C1) is a fixed-source problem with a linearly anisotropic flux imposed on the diffusion/transport interface and that the fission source (if there exist fuel materials in the transport domain) is scaled by the global eigenvalue. Both the

external incoming flux at the diffusion/transport interface and the global eigenvalue are provided by the diffusion method. Once Equation (C1) is solved, the albedo coefficients will be calculated as the ratio of the outgoing partial current to the incoming partial current on the diffusion/transport interface. These albedo coefficients are then repeatedly used by the diffusion method to do more accurate calculations in the diffusion domain. The iterations between the diffusion and transport methods are continuously performed until both the eigenvalue and albedo coefficients on ∂V_{DT} are converged.

b2. RESPONSE-FUNCTION-BASED TRANSPORT METHOD

As mention in the above section, during the diffusion/transport iterations, equation (c1) is repeatedly solved once the diffusion method provides the updated interface condition (the incoming flux on the diffusion/transport interface). The incident flux response expansion method [2] is an ideal candidate to obtain the transport solution to Equation (c1) because of its high accuracy and computational efficiency. By this approach, the transport domain V_T is first divided into a number of non-overlapping coarse meshes $\{V_i\}$. Based on the incident response flux expansion method, the outgoing partial current (and its higher moments) from a coarse mesh can be written as the superposition of all contributions responding to each incoming partial current entering from the adjacent coarse meshes:

$$J_s^{+,m} = \sum_{m',s'} R_{s's}^{m'm} J_{s'}^{-,m'}. \tag{C3}$$

where $J_s^{\pm,m}$ is the m[th] expansion coefficient (moment) of the outgoing/incoming current on surface s, $R_{s's}^{m'm}$ are the surface-to-surface response functions. The physical meaning of response functions is obvious: the response functions $R_{s's}^{m'm}$ are the magnitude of the m^{th} moment of the outgoing partial current crossing surface s as the response to a unit incoming partial current in the m'^{th} mode through surface s'. Essentially, the response functions of a coarse mesh are the solutions to a local fixed-source problem with a predefined incoming flux imposed on one of the bounding surfaces. For example, the surface-to-volume response functions $R_{is}^m\left(\vec{r},\hat{\Omega},E\right)$ are the solution to the following local transport problem.

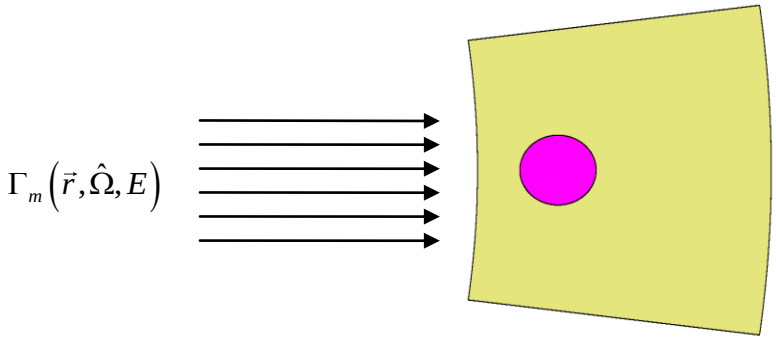

Figure C1: Local geometry for response function generation

$$\mathbf{H}R_{is}^m\left(\vec{r},\hat{\Omega},E\right) = \frac{1}{k}\mathbf{F}R_{is}^m\left(\vec{r},\hat{\Omega},E\right) \quad \vec{r} \in V_i \tag{C4}$$

with the boundary condition

$$R_{is}^{m}\left(\vec{r},\hat{\Omega},E\right)=\begin{cases}\Gamma_{m}\left(\vec{r},\hat{\Omega},E\right) & \text{on surface } s \ \ \& \ \ \hat{\Omega}\cdot\vec{n}<0\\ 0 \quad \text{on } \partial \mathrm{V_i} \text{ but not on surface } s & \& \ \ \hat{\Omega}\cdot\vec{n}<0\end{cases} \tag{C5}$$

where $\Gamma_{m}\left(\vec{r},\hat{\Omega},E\right)$ are the orthogonal expansion functions which are defined in the next subsection. There is the following relation between the surface-to-surface and surface-to-volume response functions.

$$R_{s's}^{m'm}=\int_{S}ds\int_{4\pi}d\hat{\Omega}\int dE\left(\hat{n}^{+}\cdot\hat{\Omega}\right)\Gamma_{m}\left(\vec{r},\hat{\Omega},E\right)R_{is'}^{m'}\left(\vec{r},\hat{\Omega},E\right). \tag{C6}$$

b3. Expansion Functions

Conventionally, the tensor-product of Legendre polynomials is used as orthogonal expansion functions to expand the flux distributions on the interfaces between coarse meshes [3-6]. However, the previous research has shown that they would introduce singularities in the scalar flux on the coarse mesh interface and consequently cannot be used to couple with the diffusion method. The angular expansion functions developed in reference 1 will be used in this work.

$$\Gamma_{ijg}\left(\vec{r},\hat{\Omega},E\right)=\bar{P}_{i}\left(\vec{r}\right)\psi_{j}\left(\hat{\Omega}\right)\delta_{g}\left(E\right) \tag{C7}$$

where $\bar{P}_{i}\left(\vec{r}\right)$ are the scaled Legendre polynomials, and the 0^{th} and 1^{st} order angular expansion functions are defined as:

$$\begin{aligned}&\psi_{0}\left(\hat{\Omega}\right)=1,\\ &\psi_{1}\left(\hat{\Omega}\right)=3\sqrt{2}\sin\theta\sin\varphi-2\sqrt{2},\\ &\psi_{2}\left(\hat{\Omega}\right)=2\sin\theta\cos\varphi\\ &\psi_{3}\left(\hat{\Omega}\right)=2\cos\theta\end{aligned} \tag{C8}$$

where $\psi_{0}\left(\hat{\Omega}\right)$ represents the isotropic expansion function, $\psi_{1}\left(\hat{\Omega}\right)$, $\psi_{2}\left(\hat{\Omega}\right)$ and $\psi_{3}\left(\hat{\Omega}\right)$ represent the linear anisotropic flux in the radial (*r*-axis), tangential (Θ-axis) and axial (*z*-axis) directions.

b4. Numerical Procedures

The flowchart of the diffusion/transport method is schematically illustrated in Figure C1. The transport component of the hybrid method consists of the tree numerical steps: response function generation, iterative sweeping to compute the partial currents crossing the coarse mesh interfaces, and local calculations of the flux distribution within each transport node and the albedo coefficients on the diffusion/transport interface.

In the first step, MCNP was modified to solve the local problem (C4) to obtain response functions for each unique coarse mesh. The Monte Carlo method is chosen to generate the response function library because of its geometric flexibility. It can be seen from Equation (C4) that the response functions also depend on the core eigenvalue for fuel regions. The response functions can be calculated in a set of predefined eigenvalues (e.g. 0.95, 1.0 and1.05). These calculations are performed in the pre-computation phase. In addition, since the response calculations are generated by solving local fixed problems for a small region (each unique coarse mesh) with the vacuum boundary, these pre-computations are very efficient for all regions. Therefore the computational time is not a concern.

In the second step, a deterministic sweeping method can be used to iteratively determine the partial current crossing the transport nodes. The sweeping procedure is started from the transport nodes which are next to the diffusion and transport interface. The incoming fluxes (or partial currents) provided by the diffusion method are used as an external source impinging on the transport domain. The particle balance equation (C3) is used to repeatedly calculate the outgoing partial currents from each transport node. The above mentioned inner iterations must be repeated until the outgoing partial current from each transport coarse mesh is converged.

Once the inner iterations are converged, the flux distribution within each transport coarse mesh can be easily computed as a superposition of all contributions responding to each incoming flux entering from the adjacent coarse meshes.

$$\psi_i\left(\vec{r},\hat{\Omega},E\right)=\sum_{m,s}J_s^{-,m}R_{is}^{m}\left(\vec{r},\hat{\Omega},E\right)\qquad \vec{r}\in V_i \tag{C9}$$

The albedo coefficients on the diffusion/transport interface are calculated as the ratio of the outgoing partial current to the incoming partial current. These albedo coefficients are then iteratively used by the diffusion method to perform core calculations in outer iterations. It should be pointed out that the transport method can provide the higher moments to the diffusion method if necessary.

D. Task 1.4: Test product of 1.3 on an existing 2D benchmark problem, *Georgia Tech/INL*

1. Task Status and Significant Results

   a. Task Summary

   The aim of this task is to test and validate the integrated diffusion/transport (IDT) method on a benchmark problem by comparing the IDT calculations with MCNP reference solutions.

   b. Task Status/Progress

   b1. Test of the transport module

   In order to test the accuracy of the response-function-based transport method, a direct comparison with the MCNP reference solution was performed.

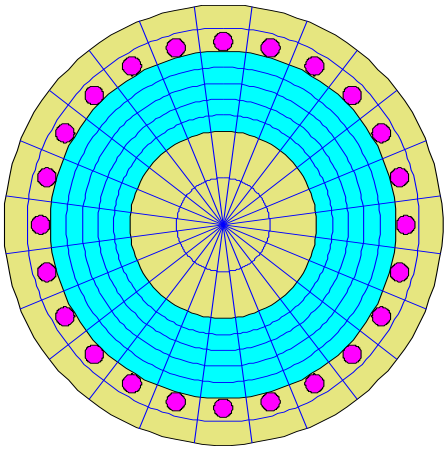

Figure D1. Geometric configuration of the 2-D benchmark problem

The 2-D Pebble Bed Reactor (PBR) benchmark problem, shown in Figure D1, consists of an inner reflector region with a diameter of 2 meters (m), a homogeneous annular fuel region of 0.85 m thickness and a 0.5 m thick controlled outer reflector region. There are 24 control rods made of B_4C each of 0.2 m in diameter whose centers are evenly positioned on a circumference of a 3.902 m diameter ring. Vacuum boundary condition is imposed on the outer cylindrical surface.

Two different control states were selected to test the transport method: core 1: 12 rods are inserted in every other rod location, and core 2: 12 rods randomly inserted (rods 1, 2, 4, 8, 9, 12, 16, 17, 18, 21, 22 and 23 are placed).

The local transport method is used in the entire outer reflector in which the diffusion approximation is not sufficient. In this test, MCNP was first used to perform the whole-core benchmark calculation using 2-group cross sections. In order to test the accuracy of the local response-funciton-based transport method only, the MCNP scalar fluxes and net currents on the fission/outer reflector interface were used as the incoming sources to perform a response-function-based transport calculation for the problem consisting of the outer reflector and control ring as shown in Figure 4. Note in the local transport calculations, the outgoing flux escaping from the transport domain (the entire outer reflector) is assumed to never come back, i.e. the fuel region and inner reflector are treated as an infinite absorb.

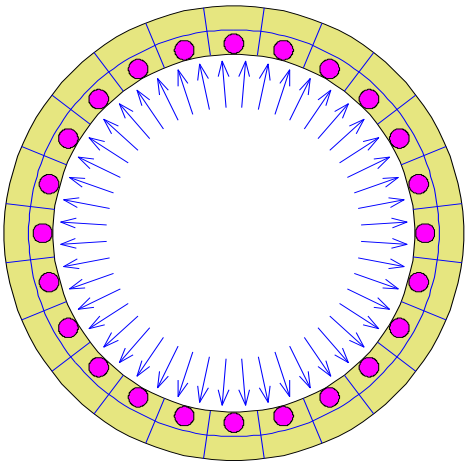

Figure D2. Local response-function-based transport calculation model

The quantities of interest in the comparison is the average relative difference (AVE), root mean square (RMS), mean relative difference (MRD) and maximum (MAX) relative difference of the node-averaged fluxes computed by the two methods. These statistical quantities for the two benchmark problems are listed in Table I. The comparison of the node-averaged fluxes in the outer reflector against the MCNP reference solution is also illustrated in Figs. D3-D6. In the response- function-based transport calculations, the spatial and angular expansion orders are 4 and 1, respectively.

Table DI. statistics of the relative difference between the node-averaged fluxes predicted by the two methods

Core State		AVG (%)	MRD (%)	RMS (%)	MAX (%)
Core 1	Fast	0.17	0.17	0.20	0.52
	Thermal	0.19	0.19	0.24	0.56
Core 2	Fast	0.13	0.12	0.17	0.55
	Thermal	0.21	0.13	0.28	0.72

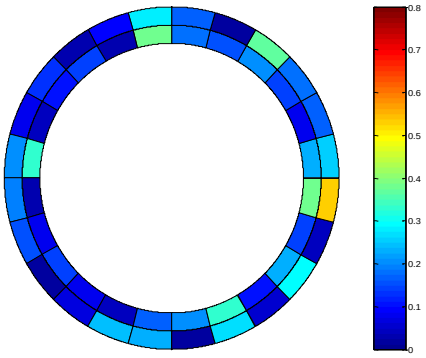

Figure D3. Relative difference (%) of the fast node-averaged fluxes predicted by the two methods for core 1 (control rod is placed in every other location)

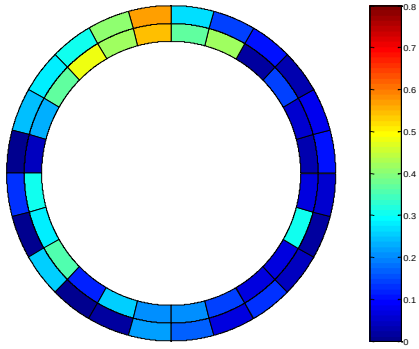

Figure D4. Relative difference (%) of the thermal node-averaged fluxes predicted by the two methods for core 1 (control rod is placed in every other location)

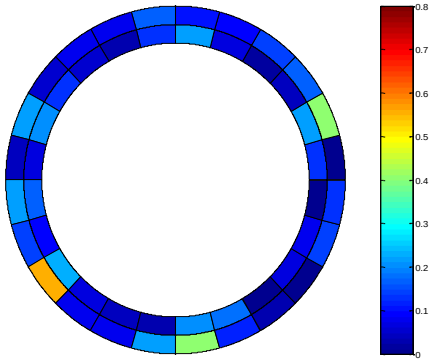

Figure D5. Relative difference (%) of the fast node-averaged fluxes predicted by the two methods for core 2 (12 control rods are randomly inserted)

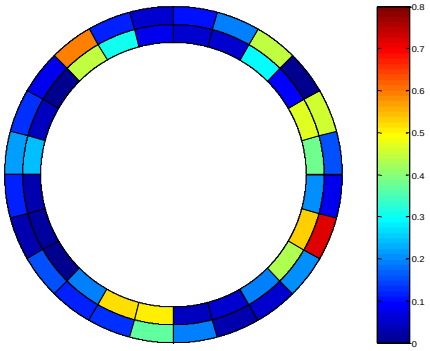

Figure D6. Relative difference (%) of the thermal node-averaged fluxes predicted by the two methods for core 2 (12 control rods are randomly inserted)

From the comparisons it can be seen that both the fast and thermal fluxes calculated by the local transport method agree very well with the MCNP reference solutions. The relative and maximum difference is about 0.18% and 0.55% for core 1. The similar agreement is found for core 2. The excellent agreement between the results of the response function method and the MCNP reference solutions indicates that a low order flux expansion can sufficiently represent the actual flux distribution on the coarse mesh boundaries and the local response-function-based method can reproduce the MCNP benchmark solutions since there is no need for the spatial homogenization.

b2. Test of the IDT method in 2D (r, theta) geometry

It is well known that large transport effects occur in the radiation field due to the presence of a control rod. In the PBMR design the control rods, which are located in the outer reflector, have a great impact on the radiation field. To account for the transport effects, a response function nodal method which can accurately model neutron transport was derived and implemented inside of a cylindrical nodal code (CYNOD).

The nodal response function method is coupled to the designated diffusion regions through scalar fluxes and net currents. The transmission of the neutron current from one designated region into the other is updated in the source iteration process in the inner iteration. The hybrid method works as follows: the averaged nodal flux and net currents at the diffusion/transport surface are calculated by the diffusion module. These scalar fluxes and net currents are used as an external source imposed on the transport nodes. The outgoing partial currents (and their higher expansion moments) are repeatedly calculated via the pre-computed response functions until they are converged. The outgoing currents from the response region at the adjoined diffusion/response boundary become a new set of inputs to the diffusion region and are incorporated into the nodal source of the adjoined diffusion nodes. The nodal sources to the diffusion region are then updated and new average nodal scalar flux values are obtained for the next source iteration. In this way the response and diffusion regions are iterated upon until the average nodal scalar flux is converged to a specified tolerance.

Results:

The hybrid method was implemented for a cylinder of infinite height. The reactor core has a total radius of 235 cm, and is made of three basic regions. The first region is an inner reflector with a radius of 100 cm, the second region is fuel ring that is 85 cm long, and the third region is an outer reflector that is 50 cm long.

The inner blue zones are the inner reflector, the green zone is the core fuel, and the red zones are the outer reflector. The deep red zone or first outer reflector region contains 24 control rods. These are equally spaced throughout the outer reflector region close to the core fuel zone. A reference solution was generated by Monte Carlo (MCNP) for comparison

Table D2: the critical core eigenvalues for a fully shutdown case with 24 control rods inserted.

Case	Core Eigenvalue
Reference	0.97515
Pure Diffusion	0.98192
Hybrid	0.97443

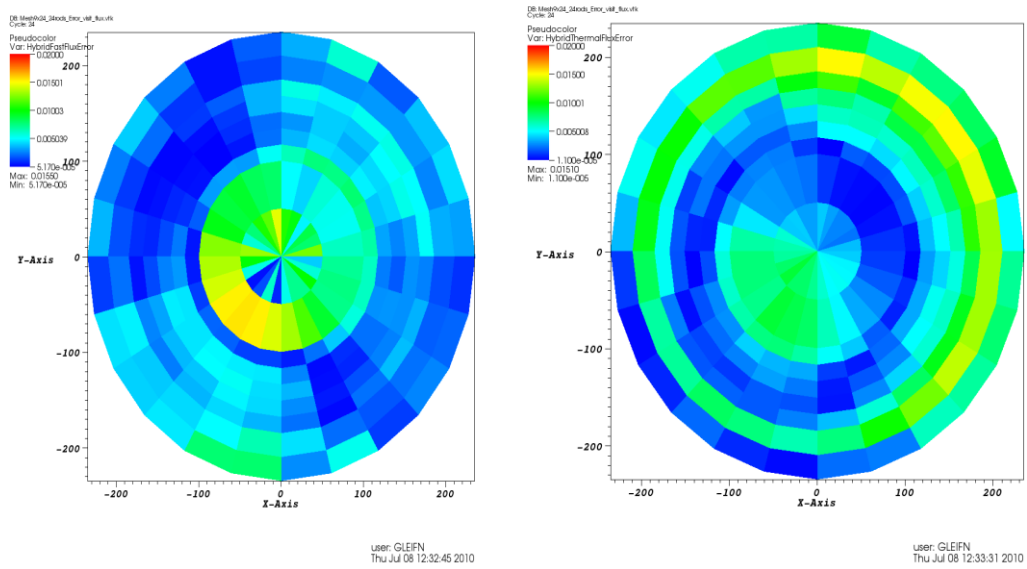

Fig. D7: Plots of the relative errors for the fast and thermal energy group scalar fluxes with 24 control rods inserted. The relative errors are obtained by comparing the scalar fluxes generated by MCNP and the fluxes generated from CYNOD Hybrid.

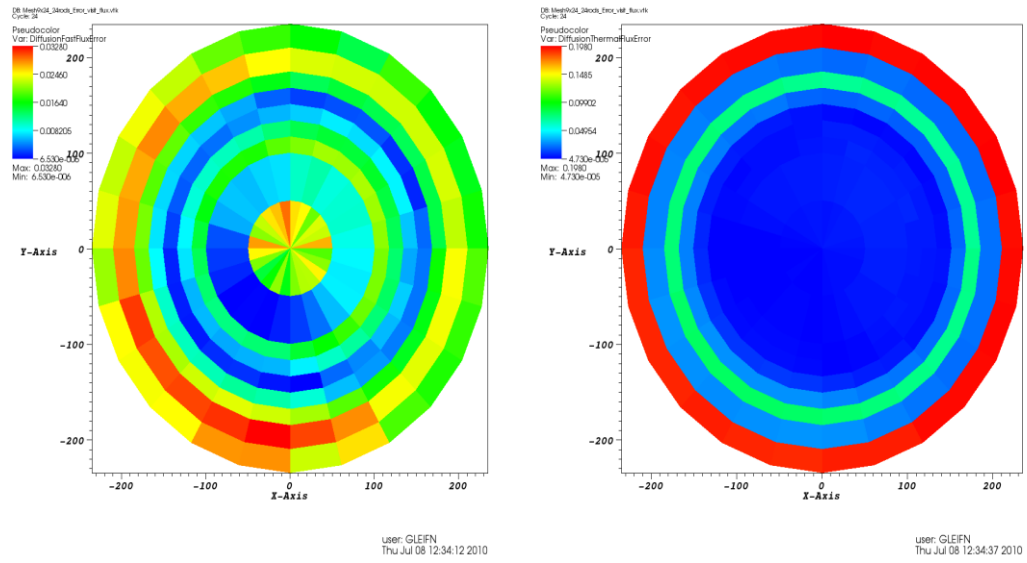

Fig.D8: Plots of the relative error of the pure diffusion solution with 24 control rods inserted. The pure diffusion solution obtained from CYNOD is compared to a MCNP solution for the fast and thermal scalar fluxes

As shown in the table above the as expected the hybrid has a critical core eigenvalue that is less than 0.08% while the pure diffusion solution is less accurate giving critical core eigenvalue that is within 0.6%.

Furthermore, in Figures D9 and D10 the relative errors of the fluxes are obtained from a comparison with MCNP are shown. As expected the relative error of the hybrid solution is much less than that of the diffusion solution. For the thermal energy group the pure diffusion solution has a relative error that is above 19% in the outer reflector while the hybrid solution is less than for all regions 2%. In the fast energy group the diffusion solution shows a relative error of about 3% in the control rod region while the hybrid solution shows a relative error less than in all regions 2%.

The hybrid methodology was also examined for twelve control rods randomly distributed in the control reflector region. Thus for this case twelve rods are randomly distributed. The critical core eigenvalues for twelve randomly distributed rods are shown in table D3.

Table D3: These are the critical core eigenvalues for 12 control rods randomly distributed.

Case	Core Eigenvalue
Reference	1.02575
Pure Diffusion	1.02555
Hybrid	1.02549

Both the diffusion and hybrid methods give critical core eigenvalues that are less than 0.03% error. Both methods obtain an excellent critical core eigenvalue. The diffusion solution does slightly well.

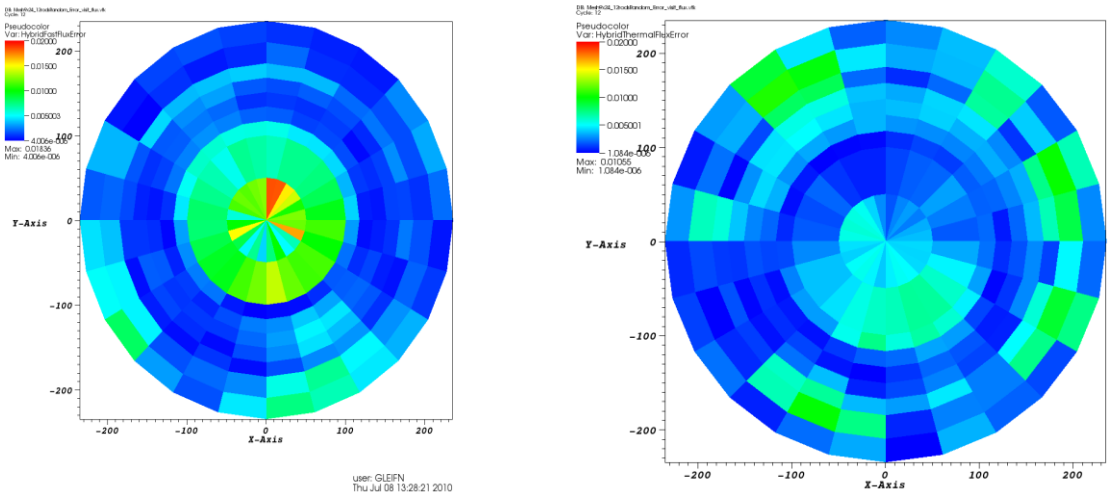

Fig.D9: Plots of the relative error for the fast and thermal fluxes for twelve randomly inserted control rods. In these plots the Hybrid method is compared to the MCNP.

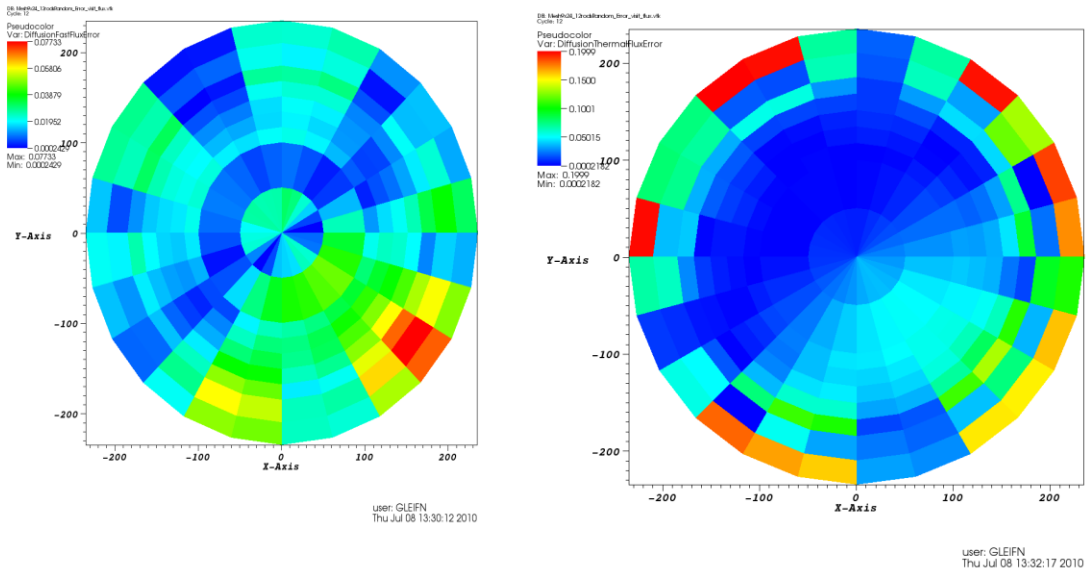

Fig. D10: Plots of the relative error of the fast and thermal fluxes with twelve control rods randomly inserted. The relative error was obtained by comparing pure diffusion CYNOD and MCNP.

However, as shown in Figures D9 and D10 the relative error of the hybrid solution is much less than that of the diffusion solution. For the thermal energy group the pure diffusion solution has a relative error that is above 19% in the outer reflector while the hybrid solution is less than for all regions 2%. In the fast energy group the diffusion solution shows a relative error of about 3% in the control rod region while the hybrid solution shows a relative error less than in all regions 2%.

E. Task 2.6: Develop, implement (into MCNP) and test the (r-z) response function-based transport method, *Georgia Tech*

1. Task Status and Significant Results

a. Task Summary

The aim of this task is to develop a 2D(r, z) transport method to generate response functions, in terms of exiting partial currents, surface-averaged and node-averaged scalar fluxes, for non-multiplying regions such as inner and outer reflectors to couple with the diffusion method. This task is essentially to develop a set of expansion functions, which is suitable for coupling with 2D(r, z) diffusion methods on the interfaces between diffusion and transport regions, to expand/approximate particle phase space distributions. These expansion functions will be used as boundary conditions to generate local solutions (i.e. response functions) for each unique coarse mesh in Task 2.7.

b. Task Status/Progress

In this performance period, we have developed a set of orthogonal expansion functions for a (*r*, z) node shown in Figs. E1 and E2.

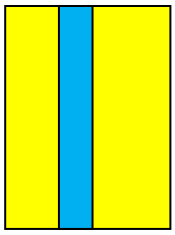

R1 R2

Figure E1: A 2D(r-z) cylindrical coarse mesh

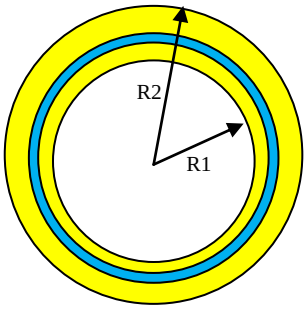

Figure E2: The (r, Θ) view of the coarse mesh shown in Fig. E1

The previously developed expansion functions, which are the tensor products of Legendre and Chebyshev polynomials, can be extended to the inner and outer cylindrical surface if the neutron direction $\hat{\Omega}$ is represented (measured) in the local geometry as illustrated in figure A3. The expansion functions can be written as:

$$f_{ijk}\left(z,\hat{\Omega}\right)=P_i(z)U_j(\cos\theta)P_k(\cos\varphi) \quad \text{on the inner/outer cylindrical surface} \qquad \text{(E1)}$$

where i, j, and k are expansion orders in spatial, polar angle and azimuthal angle, respectively. Chebyshev polynomials $U_n(\mu)$ of the second kind have the recurrence relation given below.

$$\begin{aligned} &U_0(\mu)=1 \\ &U_1(\mu)=2\mu \\ &U_{n+1}(\mu)=2\mu U_n(\mu)-U_{n-1}(\mu) \quad \text{for} \quad n\geq 1 \end{aligned} \qquad \text{(E2)}$$

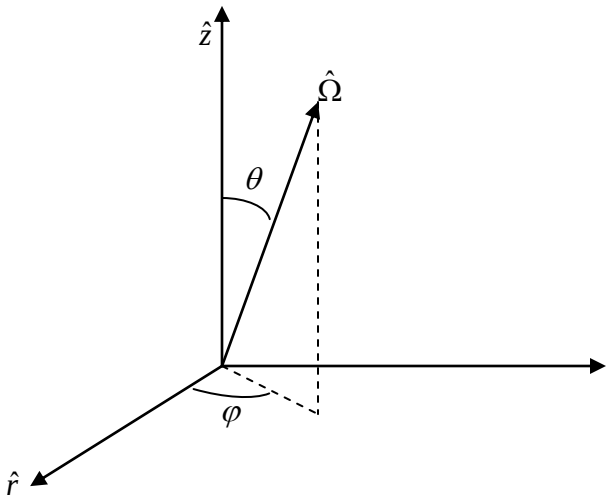

Figure E3: Local representation of $\hat{\Omega}$ on the inner/outer cylindrical surface

On the top and bottom surfaces, the same angular expansion functions can be used if the neutron direction $\hat{\Omega}$ is represented (measured) in a local geometry as illustrated in figure A4. However, in order to ensure the particle balance over the top and bottom surface, the spatial expansion functions must satisfy the following orthogonality conditions:

$$\int_{R1}^{R2} 2\pi r q_m(r) q_n(r)\, dr = A_m \delta_{mn} \tag{E3}$$

where δ is the Kronecker delta, A_m are the constants.

Obviously, Legendre polynomials cannot be used to expand the spatial distributions since they do not satisfy the orthogonality conditions E3.

Since the 0-th moment usually represents a uniform distribution over the surface, we choose:

$$q_0(r) = 1 \tag{E4}$$

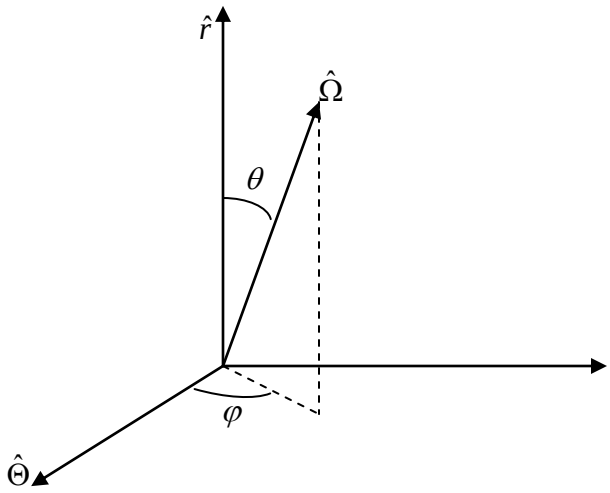

Figure E4: Local representation of $\hat{\Omega}$ on the top/bottom surface

The higher order expansion functions can be constructed as:

$$q_m(r) = rq_{m-1}(r) - \sum_{n=0}^{m-1} B_{m,n} q_n(r) \tag{E5}$$

where coefficients $B_{m,n}$ are defined as:

$$B_{m,n} = \frac{1}{A_n} \int_{R1}^{R2} 2\pi r^2 q_{m-1}(r) q_n(r) dr \tag{E65}$$

It should be pointed out that, for the inner reflector (R1=0), the above expansion function $q_m(r)$ is equivalent to Chebyshev polynomials of the first kind. However, for the outer reflectors, we must use Equations E5 and E6 to construct the expansion functions numerically.

As a result, the angular flux on the top/bottom surface can be expanded in terms of the following representation functions:

$$f_{ijk}(r, \hat{\Omega}) = q_i(r) U_j(\cos\theta) P_k(\cos\varphi) \quad \text{on the top/bottom surface} \tag{E7}$$

The above expansion functions have been implemented into the MNCP code to generate response functions for 2D(r, z) nodes. Preliminary tests have shown that the expansion functions can guarantee the particle balance.

In order to test the accuracy of the response-function-based transport method, a direct comparison with the MCNP reference solution was performed.
The 2-D (*r*, *z*) Pebble Bed Reactor (PBR) benchmark problem, shown in Fig. 5, consists of an inner reflector region with a diameter of 2 meters (m), a homogeneous annular fuel region of 0.85 m thickness and a 0.5 m thick controlled outer reflector region. The inner and outer radii of the control ring are 185.1 cm and 205.1 cm, respectively. The height in the z direction is 400 cm. The material properties for each region are listed in Table 1. Vacuum boundary condition is imposed on the outer cylindrical surface and top and bottom surfaces.

Region index	Material property
1-80	Inner Reflector
82-119, 122-159, 162-199, 202-239 and 242-279	Fuel
81, 120, 121, 160, 161, 200, 201, 240, 241, 280	Top/bottom reflector
281-320	Outer reflector with control rod
321-360	Outer reflector

Table E1: Material property of the 2-D PBR problem.

In the test, MCNP was used to perform the 2-group whole-core reference calculation. Then the MCNP reference scalar fluxes and net currents on the fission/outer reflector interface were used as the incoming sources to do a response-function-based transport calculation for the problem consisting of the outer reflector and control ring as shown in Fig. 6.

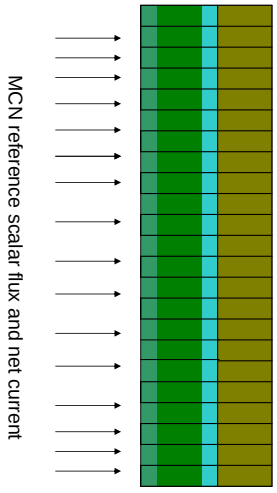

Fig. G5: Local response-function-based transport calculation model

The comparison of the node-averaged fluxes in nodes 281-360 against the MCNP reference solution are illustrated in Figs. G6 and G7. In the response- function-based transport calculation, the spatial and angular expansion orders are 4 and 1, respectively. However, the incoming surface fluxes on the interface between the fuel regions and outer reflector are assumed to be piecewise constant in space and linearly anisotropic along the radial direction (*r*-axis). As a result, the higher spatial and angular moments (including the linear angular moments in the tangential and axial directions) are ignored since the node diffusion module cannot provide such information.

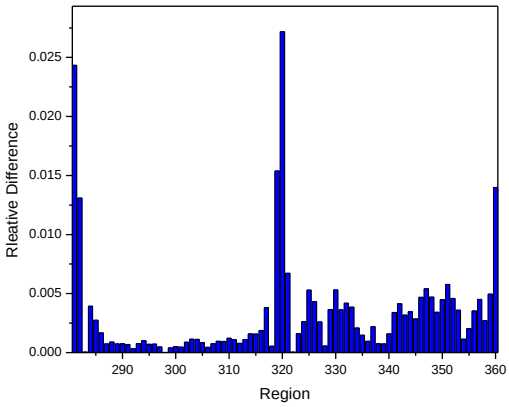

Fig. G6: Comparison of the fast node-averaged fluxes predicted by the two methods

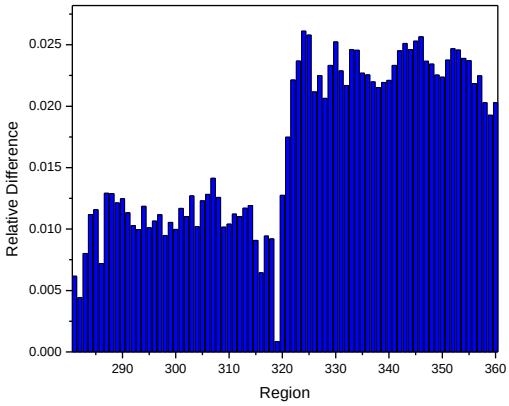

Fig. G7: Comparison of the thermal node-averaged fluxes predicted by the two methods

From Fig. G7 it can be seen that the fast fluxes calculated by the local transport method agree very well with the MCNP reference solution. The maximum errors occur in the regions close to the top and bottom boundaries. This is mainly because the high spatial moments of incoming fluxes are ignored. For the thermal flux, the relative difference varies from 0.5 to 2.5%. The slightly worse agreement of the thermal flux can be explained by the fact that the spatial gradients and high-order angular anisotropy become more import in the thermal group.

F. Task 2.7: Develop, implement and test the RMNB diffusion method, *INL*

1. Task Status and Significant Results

   a. Task Summary

   The aim of this task is to the 2D (r, z) RMNB method and to implement it into the CYNOD code.

   c. Task Status/Progress

To incorporate the response functions, the response equations of the outgoing nodal currents, the average nodal scalar flux, and the side average scalar fluxes are algebraically manipulated such that the result is a three stripe or tri-diagonal row of the average nodal scalar fluxes. This nodal response equation is then embedded seamlessly inside of the tri-diagonal matrix for the average nodal scalar flux. Iteration on the transverse leakage and nodal source terms for both diffusion and designated response nodes are done until the nodal scalar flux and net nodal boundary currents are converged.

However, a disadvantage to the direct embedding of the response functions inside the tri-diagonal matrix for the average nodal flux was the lack of higher moments in space and angle. These moments were discovered to be needed for adjoined response nodes in order to produce results with high fidelity. The direct incorporation of the higher moment equations inside the current tri-diagonal form of the flux equations would be potentially difficult and would result in a set of equations that are not in the tri-diagonal form.

To overcome these difficulties, a second approach that allowed the seamless embedding of the response equations with higher moments was devised. This new approach does not change the matrix structure of the average nodal flux, but adjoins the response region to a diffusion region through partial currents. This approach is incorporated into the nodal source iteration with the transverse leakages. The new approach works as follows: for a fixed neutron source the averaged nodal flux and net currents are calculated for the diffusion region. From the fluxes and net currents, the partial incoming currents at the adjoined diffusion/response boundary to the response region are calculated. The response region is then swept with the partial currents from the diffusion region as inputs and the partial currents in the response region are obtained. The outgoing currents at the adjoined diffusion/response boundary from the response region become a new set of inputs to the diffusion region and are incorporated into the nodal source of the adjoined diffusion nodes. The nodal sources to the diffusion region are then updated, and new average nodal scalar flux values are obtained. In this way the response and diffusion regions are iterated upon until the average nodal scalar flux is converged to a specified tolerance.

The 2D (r, z) benchmark problem described in the next section was used to test the integrated diffusion/transport method. The new approach was examined with two different couplings to the incoming current of the designated diffusion region, and in both cases the diffusion region was designated to be the inner reflector and the core region. The incoming currents to the diffusion region were obtained from albedos obtained from a reference solution in the first case, and in the second case the incoming currents were obtained from an embedded code that interacted with a segmented response function over the outer rod and reflector region. This is very close to the method implemented by Fen et al. The results of the core eigenvalue are shown in a table below.

Case	Core Eigenvalue (K_{eff})
Reference	0.90243
Pure Diffusion	0.90488
Albedos	0.90183
Embedded Response Code	0.90181

A reference solution was obtained from a MCNP model. The embedded response method and the albedos from the reference solution produce nearly the same critical core eigenvalue.

In both cases the difference between the reference eigenvalue and the calculated solution from the hybrids is 0.06%. In comparison a pure diffusion result produces a difference of 0.27%.

In addition, the nodal fluxes obtained from the embedded code and the albedos were compared against the fluxes obtained from the reference solution. As shown in Figure F2 and Figure F3 the absolute error of the average nodal flux shows good agreement with the reference solution. For the fast group in the embedded response function case the maximum error occurs around the control rod near the boundary and is less than 3.5% and for the thermal group the maximum error of the embedded response functions are less than 1.6%. The maximum error in the fast flux for the case generated with albedos is less than 3%, and the maximum error for this case in the thermal group is less than 2%. In the case generated with albedos, the diffusion region is shown since no nodal average fluxes are generated for the control rod region. These results should be contrasted with that obtained from pure nodal diffusion. For the fast energy group the relative errors are less than 3.5 % and for the thermal energy group the relative errors are up to 36.0%. This is because diffusion is well known to break down around the highly absorbing region such as a control rod.

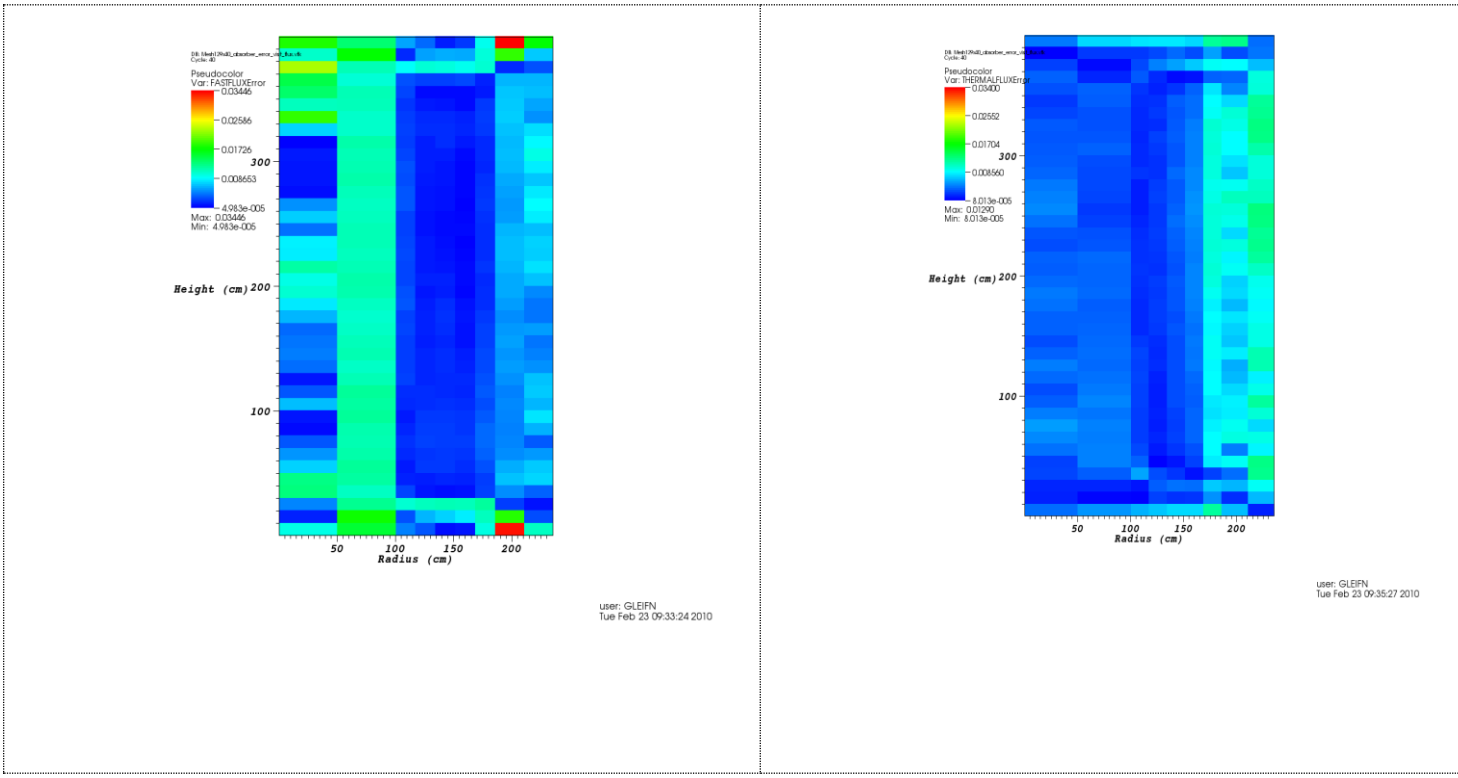

Fig. F1: Plots of the error generated by the embedded response method for the fast and thermal group average nodal fluxes.

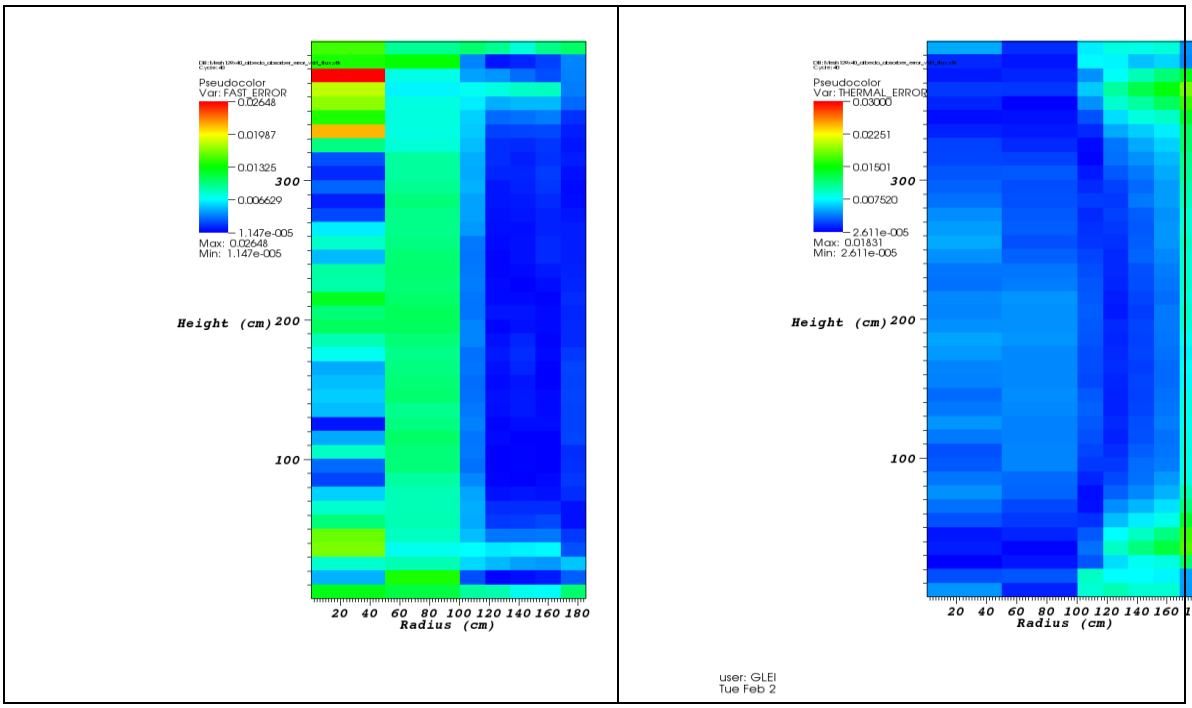

Fig. F2: Plots of the error generated by the Albedos for the fast and thermal group nodal average fluxes.

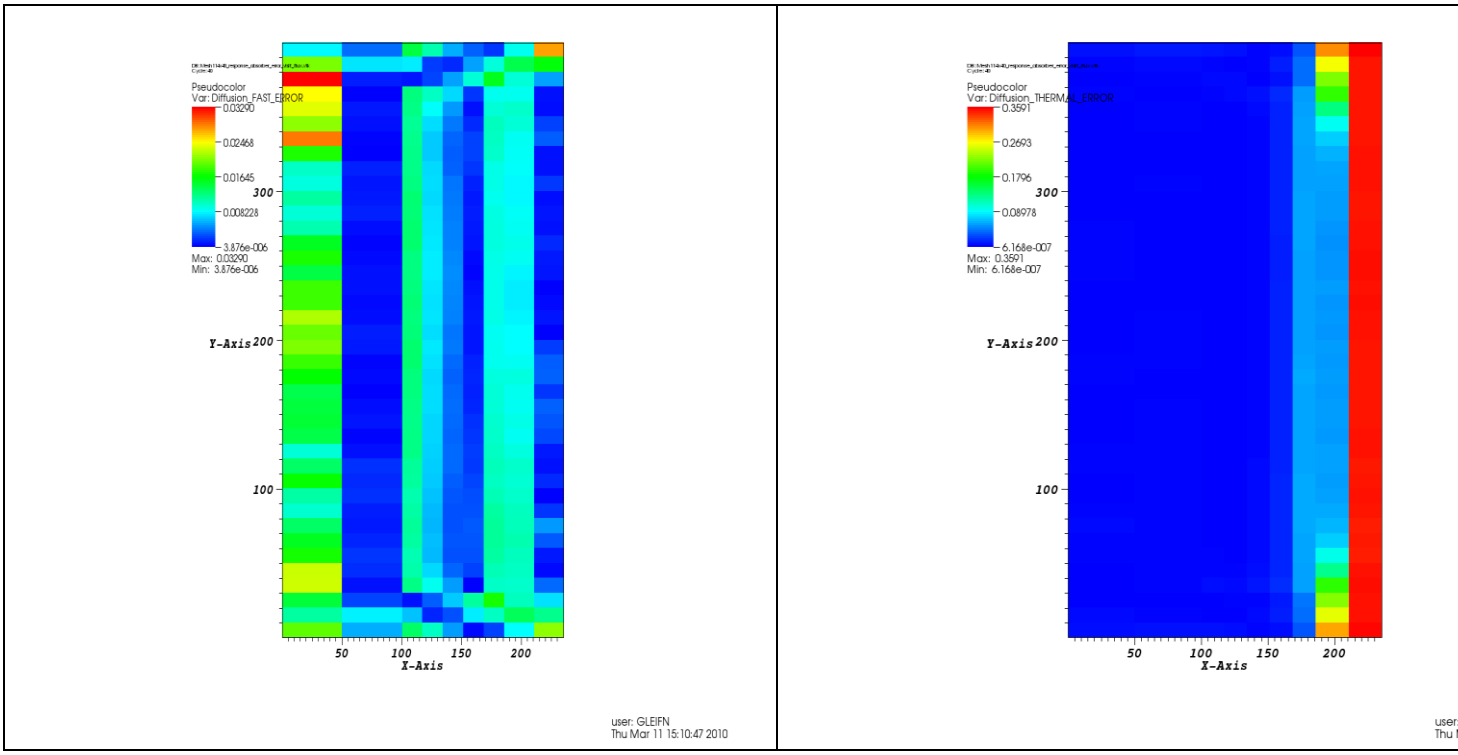

Fig. F3: Plots of the error generated by comparing MCNP results to Nodal Diffusion results for the fast and thermal group nodal average fluxes.

G. Task 2.8: Develop a PBR benchmark problem in (r-z) geometry for testing the methods in 2.6 and 2.7, *Georgia Tech*

1. Task Status and Significant Results

   a. Task Summary

   The aim of this task is to develop a PBR benchmark problem in 2D (r, z) geometry for testing the methods developed in Tasks 2.6 and 2.7.

   c. Task Status/Progress

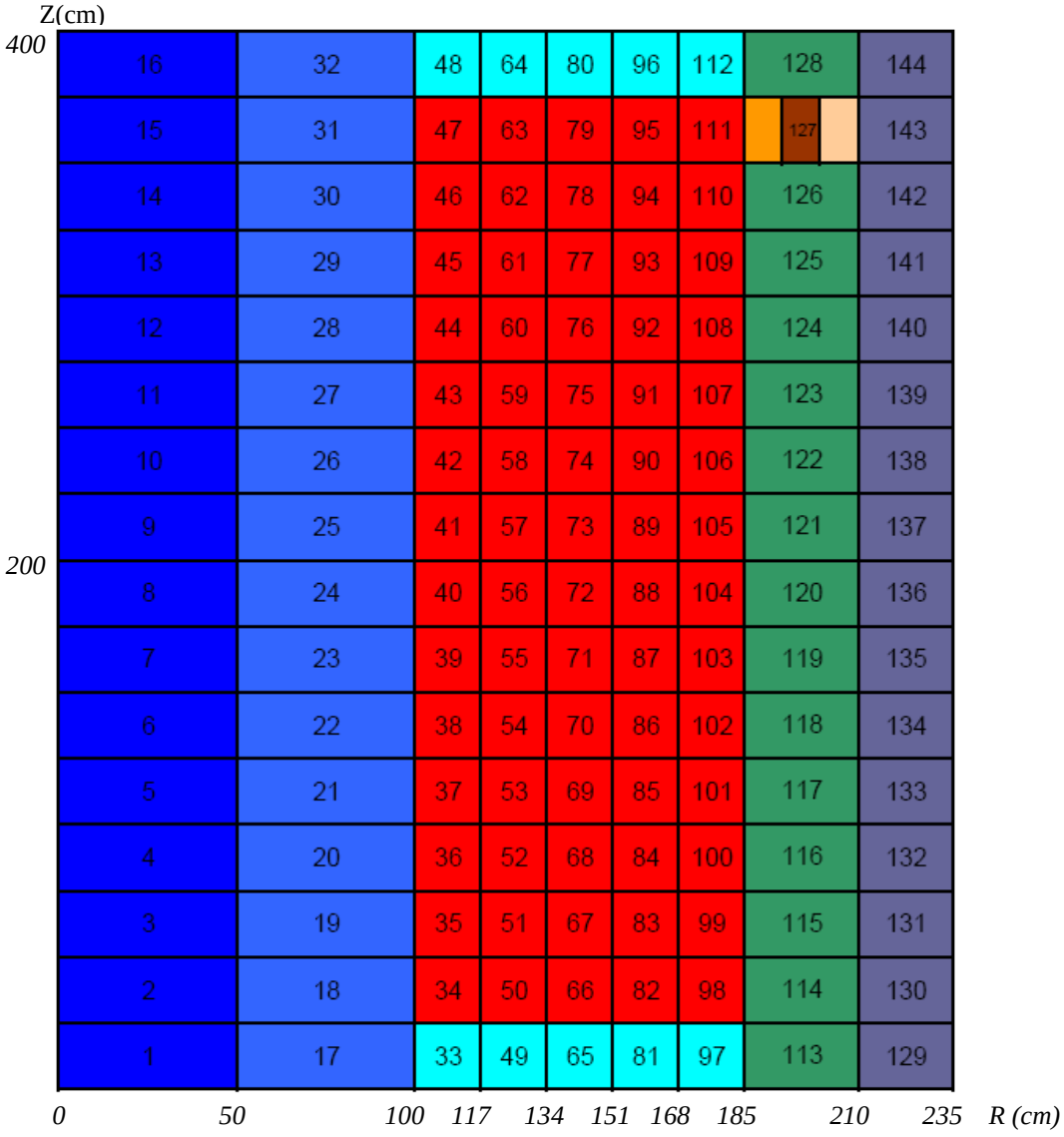

Figure G1: A 2D(R, z) PBR benchmark problem

A 2-D(r, z) PBMR 400 benchmark problem shown in Fig. G1 has been developed during this performance period. The benchmark consists of an inner reflector region with a diameter of 2 meters (m), an annular fuel region of 0.85 m thickness and a 0.5 m thick controlled outer reflector region. The height of the benchmark problem is 4 m, and the control rod is partially inserted from the top. The material for each region is listed in Table G1.

Table G1: Material composition for the 2D(r, z) benchmark problem

Region(s)	Material
1-16	Inner reflector 1
17-32	Inner reflector 2
34-47	Fuel 1
50-63	Fuel 2
66-79	Fuel 3
82-95	Fuel 4
98-111	Fuel 5
33, 48, 49, 64, 65, 80, 81, 96, 97, 112	Top/Bottom reflectors (graphite
113-126, 128	Outer reflector 1
129-144	Outer reflector 2
127	Controlled outer reflector

H. Task 2.1: Develop 3D cylindrical response function-based transport method, *Georgia Tech*

1. Task Status and Significant Results

a. Task Summary

The aim of this task is to develop a 3-D cylindrical transport method to generate response functions, in terms of exiting partial currents, surface-averaged and node-averaged scalar fluxes, for non-multiplying regions such as inner and outer reflectors to couple with the diffusion method. This task is essentially to develop a set of expansion functions, which is suitable for coupling with 3-D cylindrical diffusion methods on the interfaces between diffusion and transport regions, to expand/approximate particle phase space distributions. These expansion functions will be used as boundary conditions to generate local solutions (i.e. response functions) for each unique coarse mesh in Task 2.3.

b. Task Status/Progress

In the last performance period, we developed a set of expansion functions for a 3-D cylindrical surface, i.e. (Θ, z) surface. In this performance period, we have developed a set of orthogonal expansion functions for the other surfaces.

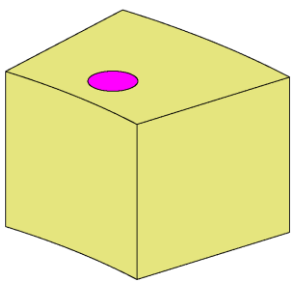

Figure H1: A 3-D cylindrical coarse mesh

We have found that the same set of expansion functions developed for the (Θ, z) surface can be extended to the (r, Θ) and (r, z) surfaces if the neutron direction $\hat{\Omega}$ is represented (measured) in local geometry as illustrated in figures H2 and H3. As a result, the expansion functions are again a tensor product of polynomials $P_n(x)$ and Chebyshev polynomials of the second kind $U_n(x)$:

$$f_{ii'jkl}\left(r,\Theta,\hat{\Omega},E\right)=P_i(r)P_{i'}(\Theta)U_j(\cos\theta)P_k(\cos\varphi)P_l(E) \quad \text{on the } (r,\Theta) \text{ surface} \qquad \text{(H1)}$$

$$f_{ii'jkl}\left(r,z,\hat{\Omega},E\right)=P_i(r)P_{i'}(z)U_j(\cos\theta)P_k(\cos\varphi)P_l(E) \quad \text{on the } (r,z) \text{ surface} \qquad \text{(H2)}$$

where i, i',j, k and l are expansion orders in spatial, polar angle, azimuthal angle and energy variables, respectively.

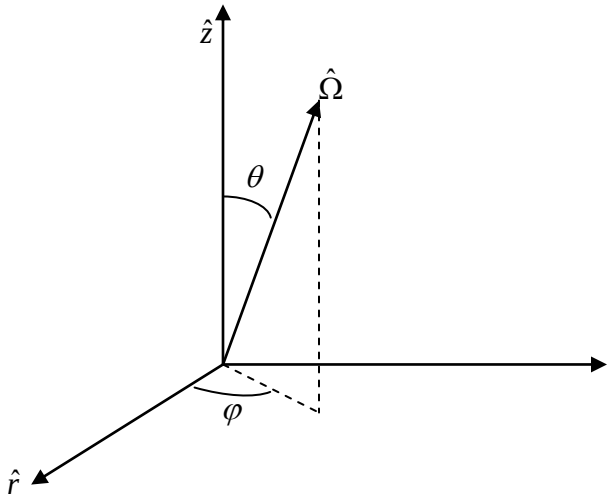

Figure H2: Local representation of $\hat{\Omega}$ on the (r, z) surface

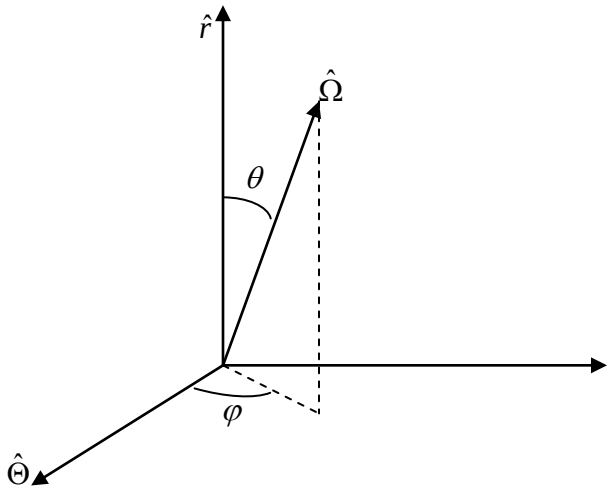

Figure H3: Local representation of $\hat{\Omega}$ on the (r, Θ) surface

I. Tasks 2.2 and 2.3: Implement results of tasks 2.1 and 2.2 into the code, *INL/Georgia Tech*

a. Task Summary

The aim of this task is to develop a 2-D hexagonal transport method to generate response functions for controlled regions to couple with the diffusion method.

d. Task Status/Progress

A 3-D sweeping module has been developed by Georgia Tech. This sweeping module uses the incoming fluxes and net currents from the diffusion code as the source to do transport calculations for the outer reflector. The albedo coefficients on the diffusion/transport surface are calculated after the partial currents crossing mesh surfaces converge. These updated albedo coefficients will then be used by CYNOD to do a diffusion calculation for the rest of the core. The MCNP reference fluxes and net currents on the fuel region/outer reflector were used to test the accuracy of the 3-D sweeping transport module. The average and maximum relative difference between the node-averaged fluxes calculated by the transport module and MCNP reference solution is about 0.8% and 4%, respectively, when the expansion orders in the two space variables and two angular (polar and azimuthal) variables are 4, 4, 2 and 2. This indicates that the transport module can achieve an acceptable accuracy at a relatively low order expansion. However, the CYNOD code uses the finite difference method (fine-mesh) in the theta direction and the mesh dimension in the z (axial) direction is required to be no more than 10 cm. This makes the sweeping module very inefficient since there are about 2,000 meshes in the outer reflector.

.

INL has implemented the transport module into the CYNOD code during the previous quarter. Accurate knowledge of the neutron radiation field is essential for the characterization of the Pebble-Bed Modular Reactor (PBMR). Efficient nodal diffusion methods provide accurate characterization of the neutron distribution, and have been successfully applied to the analysis of PBMR designs. However, these methods break down in regions that contain a control rod because of the anisotropic behavior of the neutron flux near the control rod. A new method has been developed that successfully captures the anisotropic behavior of the control rods present inside a PBMR. The method embeds a response function treatment of the control rod regions inside an accurate and efficient nodal diffusion method.

A common approach for nodal methods is to efficiently sweep the spatial mesh in a single direction, and iterate on the source. The source contains leakage information about the other transverse directions and is updated after all the net currents of the chosen direction are obtained. The new coupled approach with response functions is to incorporate the iteration over the response function region into the nodal source iteration. The approach works as follows: for a fixed neutron source the averaged nodal flux and net currents are calculated for the diffusion region. From the fluxes and net currents, the partial incoming currents at the adjoined diffusion/response boundary to the response region are calculated. The response region is then swept with the partial currents from the diffusion region as inputs and the partial currents in the response region are obtained. The outgoing currents at the adjoined diffusion/response boundary from the response region become a new set of inputs to the diffusion region and are incorporated into the nodal source of the adjoined diffusion nodes. The nodal sources to the diffusion region are then updated, and new average nodal scalar flux

values are obtained. In this way the response and diffusion regions are iterated upon until the average nodal scalar flux is converged to a specified tolerance.
The response function technique has been implemented inside of an R-Z (radial-axial) and R-Θ (radial-azimuthal) versions of CYNOD. These showed great success in capturing the effects of the control rod on the neutron radiation field. This task was to develop, implement, and test the response function method in the full 3-D (R- Θ-Z). To accomplish this task, the finite difference method was implemented for the Θ direction inside the R-Z nodal version of CYNOD. A module provided by Georgia Tech. was embedded inside this version of CYNOD, and captures the effects of the control rods by sweeping over a set of pre-computed response functions.

J. Task 2.4: Develop a 3-D PBR-VHTR benchmark problem for testing the methods in 2.6 and 2.7, *Georgia Tech*

1. Task Status and Significant Results

a. Task Summary

The aim of this task is to develop a PBR benchmark problem in 3D (r, Θ z) geometry for testing the methods developed in Tasks 2.1 and 2.2.

d. Task Status/Progress

A 3D PBMR 400 benchmark problem was developed in the performance period. The benchmark consists of an inner reflector region with a diameter of 2 meters (m), an annular fuel region of 0.85 m thickness and a 0.5 m thick controlled outer reflector region. There are 24 control rods each of 13 cm diameter whose centers are positioned on the circumference of 3.974 m diameter ring. The (r, Θ) and (r, z) cross sections of the 3D PBR problem are illustrated in Figs. J1 and J2.

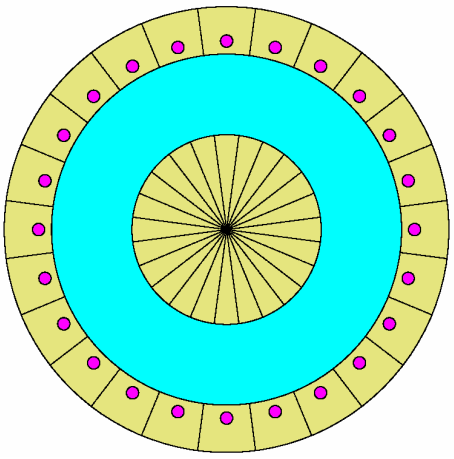

Fig. J1: (r, Θ) cross section of the 3D cylindrical benchmark problem

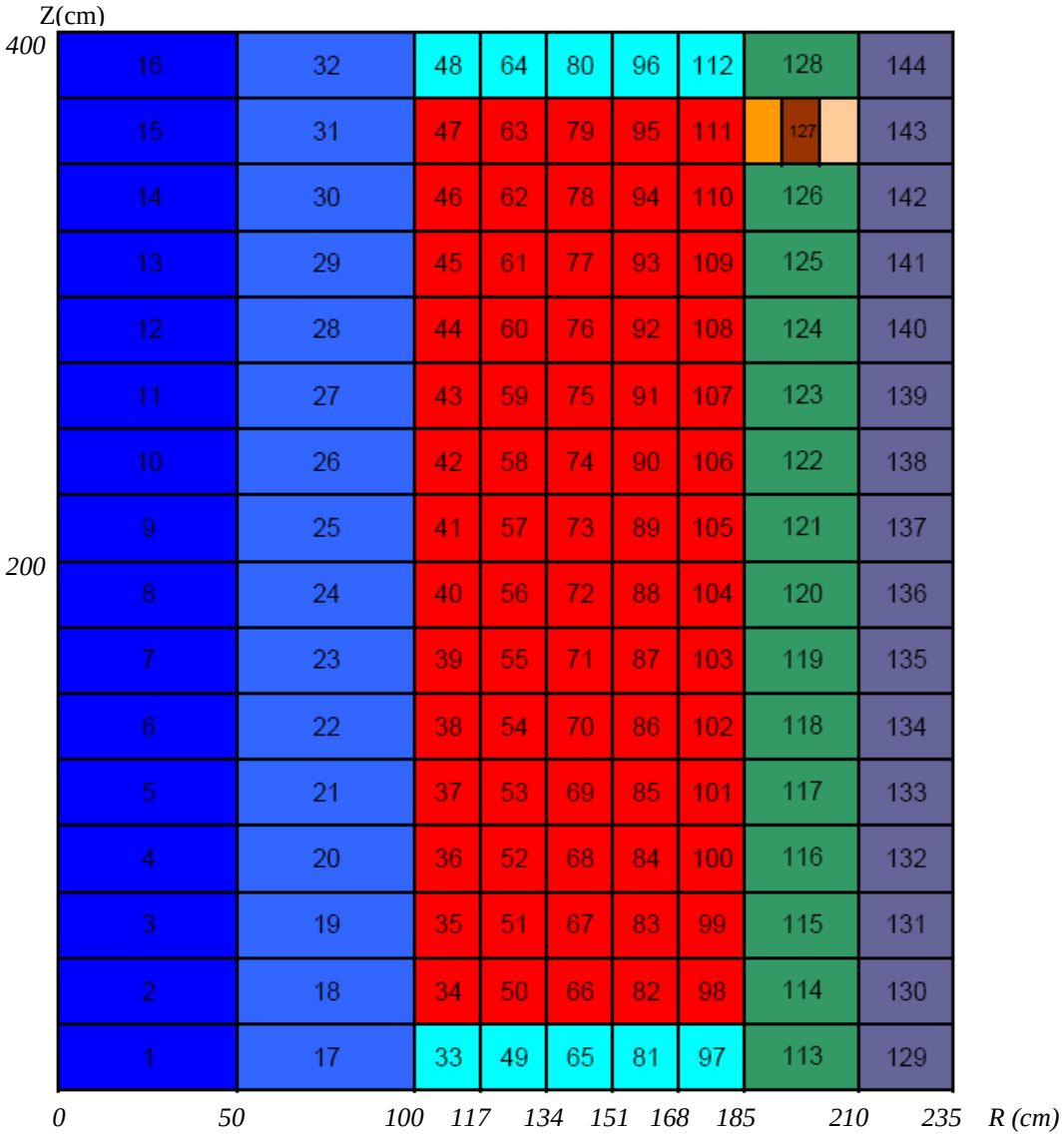

Figure J2: (r, z) cross section of the 3D cylindrical benchmark problem

2. Issues/Concerns

This task has been completed as scheduled. There are no issues/concerns.

K. Task 2.5: Test the implementation of task 2.3 with the problem in task 2.4, *Georgia Tech/INL*

1. Task Status and Significant Results

a. Task Summary

The aim of this task is to test the integrated diffusion/transport method.

e. Task Status/Progress

The method was tested on a mock pebble-bed modular reactor (PBMR) problem designed by Georgia Tech. The reactor core has a total radius of 235 cm, and is 400 cm high. The reactor core is composed of three basic regions. The first region is an inner reflector of graphite with a radius of 100 cm, the second region is fuel ring made of fuel pebbles that is 85 cm, and the third region is an outer graphite reflector that is 50 cm. A diagram of the PBMR without any control rods is shown in Figure K1. The inner blue regions are the inner reflector regions, and the yellow-orange and red regions are the outer reflector regions. The light green is the top reflector while the darker green is the pebble fuel zone.

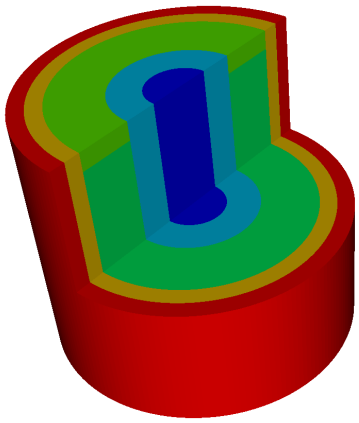

Figure K1: A diagram of the sample PBMR with no control rods

Table K1: Comparison of the core eigenvalue for the PBMR problem with no control rods

Case	Core Eigenvalue
Reference	1.0372
Pure Diffusion	1.0360
Hybrid	1.0362

Both the hybrid method and the pure nodal diffusion method are compared against a reference solution obtained from MCNP. The embedded response method and the diffusion solution produce nearly the same core eigenvalue as the reference solution.

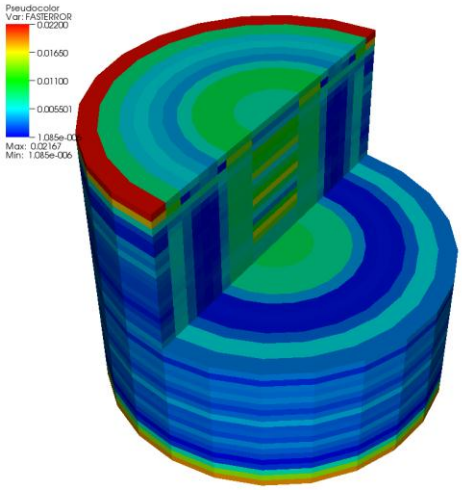

Figure K2: The relative difference in the fast fluxes between the nodal diffusion solution and the MCNP reference solution for the PBMR problem with no control rods

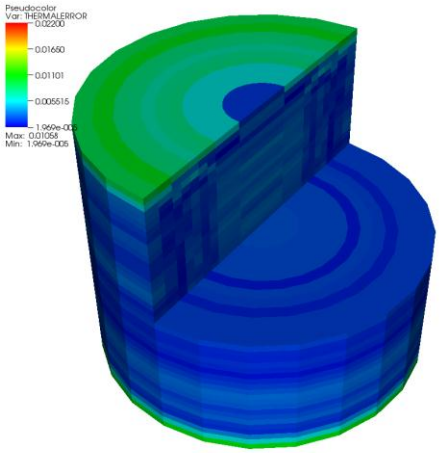

Figure K3: The relative difference in the thermal fluxes between the nodal diffusion solution and the MCNP reference solution for the PBMR problem with no control rods

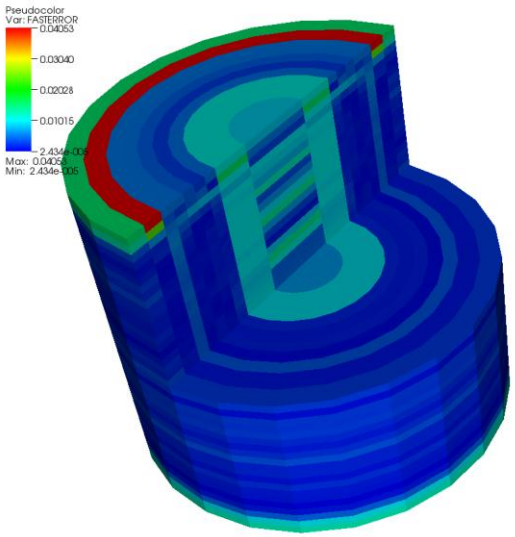

Figure K4: The relative difference in the fast fluxes between the hybrid solution and the MCNP reference solution for the PBMR problem with no control rods

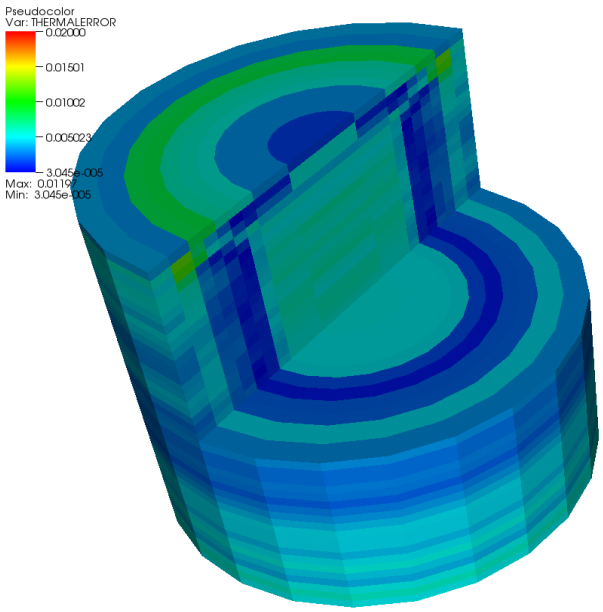

Figure K5: The relative difference in the thermal fluxes between the hybrid solution and the MCNP reference solution for the PBMR problem with no control rods

The relative errors of the nodal diffusion Fast and Thermal fluxes compared to the MCNP reference solution are shown in Figures K2 and K3, and the relative errors of the Fast and Thermal fluxes obtained hybrid method compared to the MCNP reference solution are shown in Figures K4 and K5. For the Fast flux both the pure diffusion solution and the hybrid solution have a relative error near 1% inside the reactor core. Both solutions also show a relative error a little over 2% in the inner reflector region. But, these two solutions have different regions where the maximum error occurs. The maximum relative error in the fast flux for the Hybrid solution is a little under 4.0% and occurs at the top and bottom reflectors at the inner ring. This band of error occurs because of the coupling between the response region and the nodal diffusion solver. This error may be eliminated either by refining the axial mesh near the boundary or by coupling the higher order spatial moments in the nodal diffusion solver to the higher order response function region.

Next the hybrid and pure nodal diffusion methods are tested on a PBMR core with twelve control rods evenly distributed in the inner reflector. A diagram of the PBMR with the control rods is shown in Figure K6. Like Figure K1, the inner blue regions are the inner reflector regions, and the yellow-green and orange regions are the outer reflector regions. The light green is the top reflector while the mint green is the pebble fuel zone. The red regions represent the position of the control rods inside reflector core.

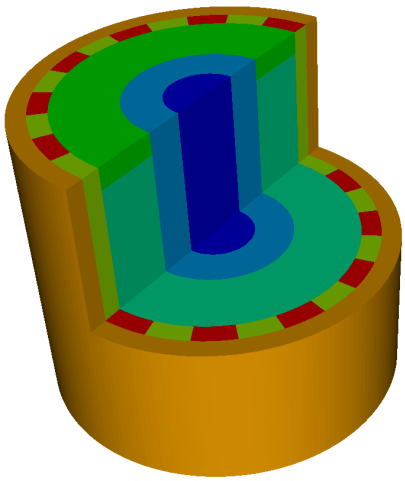

Figure K6: A diagram of the PMBR with twelve control rods evenly distributed around the inner reflector.

The critical core eigenvalue for the twelve even control rod problem are listed in Table K2. Both the pure nodal diffusion method and the response function method give critical core eigenvalues that are 0.18% less than the reference.

Table K2: These are the critical core eigenvalues for the PBMR with twelve evenly distributed control rods inserted.

Case	Core Eigenvalue
Reference	0.97805
Pure Diffusion	0.97622
Hybrid	0.97619

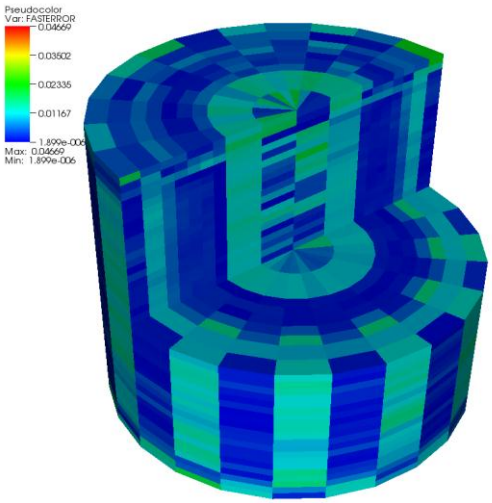

Figure K7: The relative difference in the fast fluxes between the nodal diffusion solution and the MCNP reference solution for the PBMR problem with 12 control rods evenly distributed

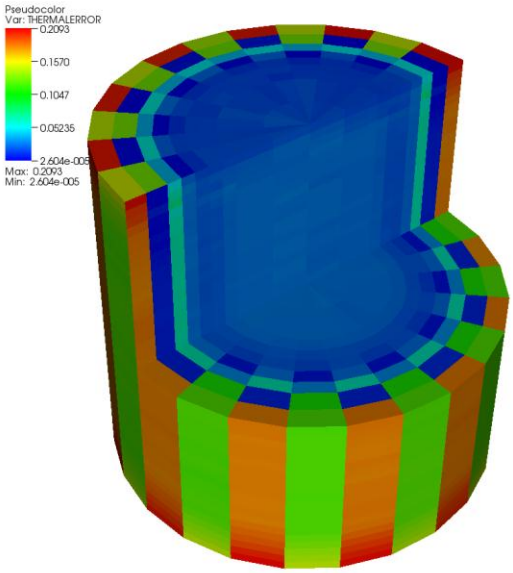

Figure K8: The relative difference in the thermal fluxes between the nodal diffusion solution and the MCNP reference solution for the PBMR problem with 12 control rods evenly distributed

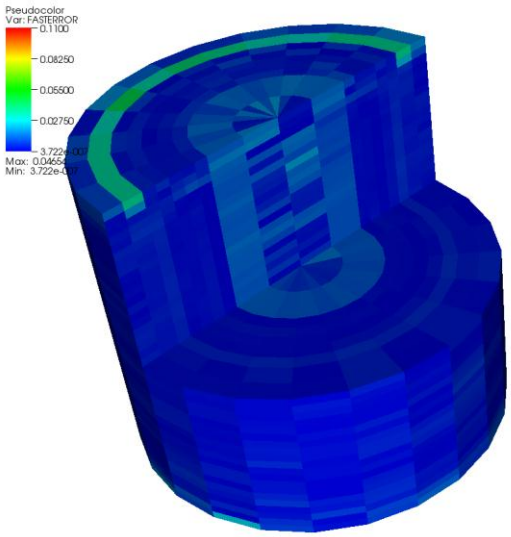

Figure K9: The relative difference in the fast fluxes between the hybrid solution and the MCNP reference solution for the PBMR problem with 12 control rods evenly distributed

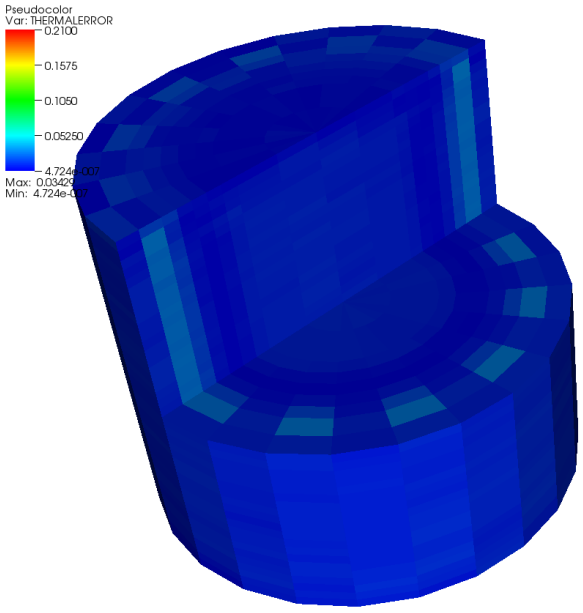

Figure K10: The relative difference in the thermal fluxes between the hybrid solution and the MCNP reference solution for the PBMR problem with 12 control rods evenly distributed

Figures K7 and K8 show the relative error obtained by comparing the nodal diffusion method to the MCNP reference solution for the reactor with twelve evenly distributed control rods. Figures K9 and K10 show the relative error obtained by comparing the reference solution to the hybrid solution. The diffusion solution shows a relative error of less than 2% in the fast flux and around 2% error in the reactor core for the thermal flux. However, the diffusion solution also has an error that is around 19% in the rodded reflector region. But, the Hybrid method shows an error of less than 2% in the fast and thermal fluxes in the core and less than 3% in the control rod region. Again a larger error band around 4.5% occurs at the boundary due to the coupling of the axial moments near the boundary.

L. Task 3.1: Develop 2D response function-based transport method for hexagonal geometry, *Georgia Tech*

1. Task Status and Significant Results

a. Task Summary

The aim of this task is to develop a 2-D hexagonal transport method to generate response functions for controlled regions to couple with the diffusion method.

b. Task Status/Progress

The transport method has been developed, implemented and tested. Over a transport region V_T, the method works as follows:

Divide the transport region V_T into a series of coarse meshes. For our purposes, each coarse mesh will correspond to a single assembly. We expand the angular flux entering each coarse mesh using an orthogonal basis.

Define the spaces of incoming ω_m^- and outgoing ω_m^+ angular flux for a hexagonal assembly V_H

$$\omega_m^{\pm} \equiv \left\{ (\vec{r},\hat{\Omega},E) \middle| \vec{r} \in \partial V_H^m, \pm(\hat{n}_H \cdot \hat{\Omega}) > 0 \right\} \tag{L1}$$

with inner products

$$\langle f,g \rangle_m^{\pm} = \int_{\partial V_H^m} d\vec{r} \int_{\pm(\hat{n}_H \cdot \hat{\Omega})>0} d\hat{\Omega} \int_0^{\infty} dE (\pm \hat{n}_H \cdot \hat{\Omega}) f(\vec{r},\hat{\Omega},E) g(\vec{r},\hat{\Omega},E) \tag{L2}$$

where ∂V_H^m is the m^{th} face of the assembly and $\hat{n}_H$ is the outward unit normal on the assembly boundary. Let $\{\gamma_0,\gamma_1,\ldots\}$ be a set of functions on ω_1^+ that are orthonormal with respect to the corresponding inner product. Note that this basis can be trivially transformed to any of the other spaces $\omega_m^{\pm}$. Let φ_i^m satisfy the fixed-source transport equation with heterogeneous boundary condition

$$\mathbf{H}_\mathbf{T}\varphi_i^m(\vec{r},\hat{\Omega},E)=\frac{1}{k}\mathbf{F}_\mathbf{T}\varphi_i^m(\vec{r},\hat{\Omega},E)\quad \text{for}\quad \vec{r}\in V_H$$
$$\varphi_i^m(\vec{r},\hat{\Omega},E)=\begin{cases}\gamma_i(\vec{r},\hat{\Omega},E), & (\vec{r},\hat{\Omega},E)\in\omega_m^- \\ 0, & (\vec{r},\hat{\Omega},E)\in\partial V_H^- - \omega_m^-\end{cases}. \tag{L3}$$

Now define the response coefficient c_{mn}^{ij}

$$c_{mn}^{ij}\equiv\left\langle\varphi_i^m,\gamma_j\right\rangle_n^+ \tag{L4}$$

to be the response of basis component j on surface n to a source of shape i on surface m. Given these coefficients and a known angular flux ψ^- impinging on the surface of the assembly, one can approximate the outgoing angular flux on surface n by

$$\psi_n^+\approx\sum_{m=1}^{6}\sum_{i,j}\gamma_j c_{mn}^{ij}\left\langle\psi^-,\gamma_i\right\rangle_m^-. \tag{L5}$$

If the basis $\{\gamma_0,\gamma_1,\ldots\}$ is complete, then the above approximation is exact in the limit as the expansion order goes to infinity. The basis must be truncated in practice, thus it is important to use a basis that provides a good representation at low order. For the spatial basis choose the orthonormal Legendre polynomials up to third order

$$\begin{aligned}p_0(x)&=\frac{1}{\sqrt{2}}\\ p_1(x)&=\frac{\sqrt{3}}{\sqrt{2}}x\\ p_2(x)&=\frac{\sqrt{5}}{2\sqrt{2}}\left(3x^2-1\right)\\ p_3(x)&=\frac{\sqrt{7}}{2\sqrt{2}}\left(5x^3-3x\right)\end{aligned} \tag{L6}$$

For the angular basis, choose the functions

$$
\begin{aligned}
q_0(\theta,\phi) &= \frac{1}{\sqrt{\pi}} \\
q_1(\theta,\phi) &= \frac{\sqrt{2}}{\sqrt{\pi}}\left(3\sin\theta\sin\phi - 2\right) \\
q_2(\theta,\phi) &= \frac{\sqrt{2}}{\sqrt{\pi}}\cos\theta\sin\phi \\
q_3(\theta,\phi) &= \frac{1}{\sqrt{17\pi}}\left(-20\sin^2\theta + 12\sin\theta\sin\phi + 7\right) \\
q_4(\theta,\phi) &= \frac{1}{\sqrt{11\pi}}\left(15\sin^2\theta\sin 2\phi - 16\sin\theta\cos\phi\right) \\
q_5(\theta,\phi) &= \frac{1}{\sqrt{34\pi}}\left(51\sin^2\theta\cos 2\phi - 47\sin^2\theta + 120\sin\theta\sin\phi - 32\right)
\end{aligned}
\tag{L7}
$$

which have been derived by orthonormalizing the spherical harmonics with respect to the inner product

$$
\langle f,g\rangle = \int_0^{\pi} d\theta\sin\theta \int_0^{\pi} d\varphi\sin\theta\sin\phi\, f(\theta,\phi)g(\theta,\phi) \tag{L8}
$$

and by omitting functions which are not symmetrical in θ about the x-y plane.

If the transport region V_T is a single assembly, then this response expansion is sufficient to provide a detailed solution. When a sub-region is composed of several adjoining assemblies, however, all of these assemblies must be coupled together to solve the transport problem. In order to solve these multi-assembly problems, an iterative sweeping method is used, where the boundary flux expansion coefficients are updated one assembly at a time until they converge. This sort of response function expansion with sweep has been shown to work well for whole-core coarse-mesh transport problems [1, 2].

The above method has been implemented. The response functions are calculated with a modified MCNP5 and post-processed with Python scripts. The iterative sweep is performed using a module written in Fortran90.

2. Issues/Concerns

   There are no issues/concerns.

M. Task 3.2: Integrate transport method from Task 3.1 with an existing diffusion method, *Georgia Tech*

1. Task Status and Significant Results

   a. Task Summary

The aim of this task is to integrate the 2-D hexagonal transport method with an existing diffusion code so that it can perform transport calculations for the selected regions while using the diffusion method for the rest of the core.

b. Task Status/Progress

PARCS has been modified to treat transport regions as external to the problem. The albedo is simply the ratio of the surface averaged net current (in the outward direction) to the surface averaged scalar flux. The unmodified PARCS uses a groupwise albedo on the external surfaces of the problem. This behavior has been modified in two ways:

- The albedo has been modified to be surface-dependent rather than having a single global albedo for each energy group.
- The input routines have been modified to treat arbitrarily placed hexagonal nodes as being external to the problem and thus treated through albedo boundary conditions.

In addition to these modifications of the albedo, PARCS has also been modified to accept a corner point ratio (CPR) boundary condition. At each corner point along the diffusion-transport interface, we specify the ratio of the scalar flux at that point to the sum of the node-averaged scalar fluxes over the entire diffusion region. This boundary condition is applied during the PARCS corner point balance. The combination of CPRs. and albedos creates a higher order boundary condition than would be possible with albedos alone.

The albedos and CPRs along the diffusion transport interface are not known *a priori*; instead, they are calculated iteratively. For an initial guess, the albedos are initialized to 0 and the CPRs are set to the reciprocal of the number of diffusion nodes. This guess would be exact in the case of an infinite medium (ie flat flux) solution. At each iteration these interface conditions are improved by a fixed source calculation in the transport region using the incident flux response expansion method. The transport method takes the incoming flux from its shared boundary with the diffusion region as input. The transport region then calculates the detailed solution that results from this diffusion surface source. From this detailed solution in the transport region, the albedos and CPRs are updated.

The incoming surface source for the transport response calculation is derived from the Triangular Polynomial Expansion Nodal (TPEN) solver in PARCS. The TPEN method (a part of the PARCS nodal update) considers each hexagonal assembly to be made of 6 triangles. It assumes that the flux shape in each triangle conforms to a 9-term polynomial

$$\phi_{TPEN}(x,y) = c_0 x + a_x x + a_y y + b_x x^2 + b_u u^2 + b_p p^2 + c_x x^3 + c_u u^3 + c_p p^3$$

$$\text{where} \quad u = \left(-x - \sqrt{3}y\right)/2 \quad \text{and} \quad p = \left(-x + \sqrt{3}y\right)/2.$$

The coefficients of the angular flux expansion described above in Task 3.1 can be calculated analytically from the TPEN coefficients. This relationship was derived analytically using the Maxima computer algebra system. These coefficients are then fed into the response functions (outlined in Task 3.1). The response is then used to update the boundary albedo and corner point ratios.

In summary, the incoming boundary conditions for the transport region are derived from the latest diffusion iteration, and then transport region response function is applied to update the diffusion boundary conditions. This interface condition update occurs after each PARCS nodal update.

2. Issues/Concerns

There are no issues/concerns.

N. Task 3.4: Test result of 3.2 with the problem of 3.3, *Georgia Tech*

1. Task Status and Significant Results

a. Task Summary

The aim of this task is to test the combined diffusion-transport method developed in tasks 3.1 and 3.2 with the HTTR benchmark developed in task 3.3.

c. Task Status/Progress

The method has been applied to a simplified version of the HTTR benchmark developed in task 3.3.

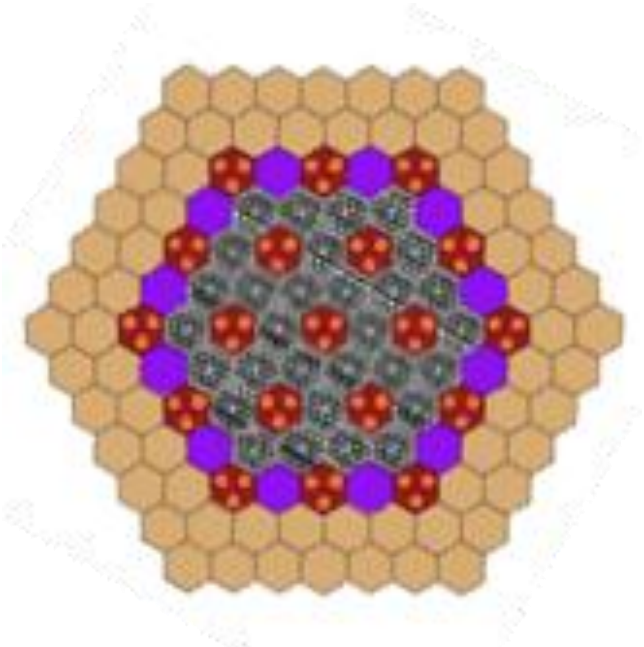

Figure N1. HTTR Core Layout

The test problem we have used differs from the one developed in 3.3 in the following ways:

- only a single type of fuel assembly is retained
- only a single type of graphite block is retained
- 2 energy groups are used instead of 6

A reference calculation is performed with MCNP5. This is compared to a whole-core diffusion calculation (denoted PARCS), and to two different diffusion-transport hybrid setups. 1) The transport region is chosen to consist of all of the control blocks; this is denoted *IDT C*. In this case, the transport region is a set of isolated blocks. 2) The transport region is chosen to be a single contiguous region consisting of all of the control blocks and all of the reflector blocks; this is denoted *IDT C+R*.

The reference eigenvalue is k=0.63536 with estimated uncertainty of 2 pcm at the 1-standard-deviation level. All of the assembly power values for the reference solution have uncertainty of less than 0.01% at the 1-standard-deviation level. Let $r_j \equiv (\tilde{p}_j - p_j^*)/p_j^*$ denote the relative error in assembly power where p_j^* is the fission rate in assembly j from the reference solution, and $\tilde{p}_j$ is the corresponding value from an approximate calculation. Table N1 compares the accuracy of the methods with respect to eigenvalue and assembly powers. Table N2 compares the computation times of the methods.

Table N1. Error comparison.

	PARCS	IDT C	IDT C+R
error in eigenvalue k (pcm)	-3303	213	183
average relative error = $\frac{1}{N}\sum_{j=1}^{N}\lvert r_j\rvert$	0.88%	0.72%	1.53%
RMS relative error = $\sqrt{\frac{1}{N}\sum_{j=1}^{N} r_j^2}$	0.97%	0.83%	1.78%
maximum relative error = $\max_j(\lvert r_j\rvert)$	1.60%	1.59%	2.69%

Table N2. Computation times on 2GHz CPUs.

Computation	Parallel Time (seconds)	Number of Cores	Seqential Time (core-seconds)
MCNP Reference Solution	4.9E+4	32	1.6E+6
Fuel Homogenization	1.7E+4	32	5.4E+5
Control Homogenization	7.7E+3	32	2.5E+5
Control Response Pre-Computation	1.3E+4	96	1.2E+6
Reflector Response Pre-Computation	7.2E+3	96	6.9E+5
PARCS	1.3E-1	1	1.3E-1
IDT C	4.7E+0	1	4.7E+0
IDT C+R	3.6E+0	1	3.6E+0

Figure N3 gives the assembly powers from the reference solution and the corresponding relative errors for the PARCS calculation and for the IDT calculations.

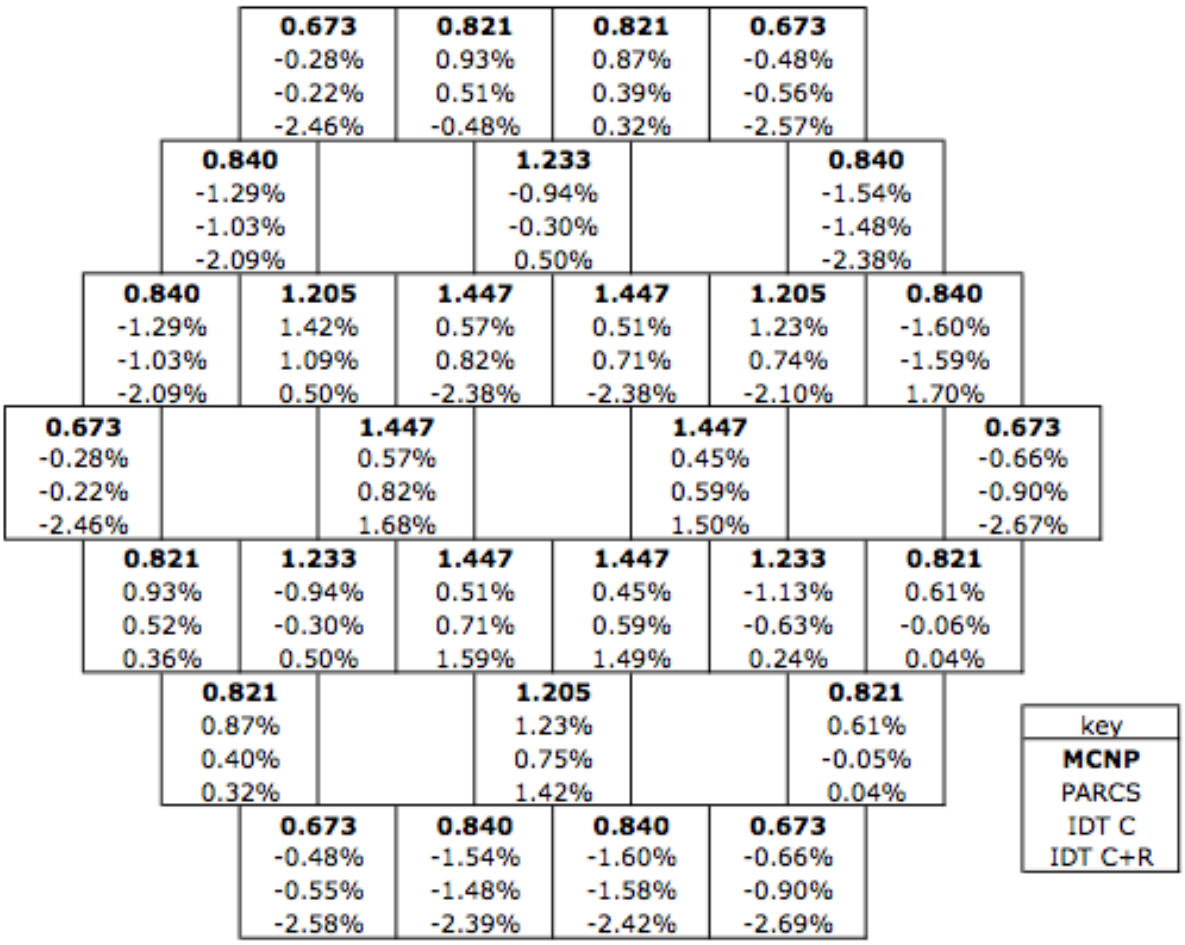

Figure N3. Assembly-wise power distribution; MCNP reference values are normalized so that the average assembly power is 1.

Both of the IDT calculations produce an eigenvalue estimate that is an order of magnitude better than that of the PARCS estimate. The best assembly powers were calculated by the IDT C computation, while the worst were with the IDT C+R computation. Both hybrid computations are nearly 6 orders of magnitude faster than the reference MCNP.

2. Issues/Concerns

This task has been performed with a simplified benchmark problem not due to any limitations of the method itself, but because we did not have access to the GenPMAXS code that is used to generate PMAXS cross section files for PARCS. Using the 2-group structure, cross sections can be input directly into PARCS, but going to a higher number of groups (6 for the problem in task 3.3) requires the PMAXS input files.

V. SUMMARY AND CONCLUSIONS

Status Summary of NERI Tasks

Milestone/Task Description (Organization)	Planned Completion Date	Actual Completion Date	Percent Complete
1.1: 2D(r, θ) response function method - GT	02/25/2008	02/25/2008	100%
1.2: 2D(r, θ) RMNB diffusion method - INL	02/25/2008	09/30/2008	100%
1.3: Implement the 2-D methods into the code - INL/GT	08/25/2008	06/30/2010*	100%
1.4: 2D PBR benchmark test – INL/GT	08/25/2008	06/30/2010*	100%
2.1: 3D(r, θ, z) response function method – GT	02/25/2009	02/25/2009	100%
2.2: 3D(r, θ, z) RMNB diffusion method - INL	11/30/2010	06/30/2010	100%
2.3: Implement results 2.1 and 2.2 into the code - INL/GT	12/30/2010	12/30/2010	100%
2.4: Develop a 3D PBR-VHTR benchmark problem - GT	09/30/2009	09/30/2009	100%
2.5: Test the implementation of task 2.3 with the problem in task 2.4 – INL/GT	12/30/2010	12/30/2010	100%
2.6: Develop, implement and test the (r-z) response function-based transport method – GT	06/30/2009	06/30/2009	100%
2.7: Develop, implement and test the RMNB diffusion method – INL	08/30/2009	06/30/2010	100%
2.8: Develop a PBR benchmark problem in (r-z) geometry for testing the methods in 2.6 and 2.7 – GT	05/31/2009	05/31/2009	100%
3.1: Develop 2D response function-based transport method for hexagonal	09/30/2010	09/30/2010	100%

geometry – GT			
3.2: Integrate the transport method into an existing diffusion code - GT	10/30/2010	11/30/2010	100%
3.3: Develop 2D prismatic VHTR benchmark problem - GT	08/30/2010	08/30/2010	100%
3.4: Test result of 3.2 with the problem of 3.3 - GT	12/30/2010	12/30/2010	100%
3.5: Write the user's manual for the modified CYNOD – INL	12/30/2010	12/30/2010	100%

* Tasks 1.3 and 1.4 were reactivated in Y3Q3 and completed in Y3Q4.

The objective of this research project was to develop an integrated diffusion/transport (IDT) method to substantially improve the accuracy of nodal diffusion methods for the design and analysis of Very High Temperature Reactors (VHTR). In this method, the reactor core is first divided into two domains: transport and diffusion domain. The traditional diffusion method is used for the region where the diffusion approximation is sufficient, while a local transport method based on the incident flux response expansion method is used for the rest of the core. Researchers implemented the method into a computer code which is capable of performing realistic whole core neutronic calculations. The method has been benchmarked extensively in benchmark configurations typical of PBR and prismatic (in 2-D) VHTR cores. Excellent accuracy against full core Monte Carlo results is achieved with the new IDT method. The hybrid whole core calculations are found to be highly accurate and very efficient.

Based on the encouraging results and efficiency obtained in this project it recommended to extend this method to three-dimensional hexagonal geometries. This will results in a highly accurate and efficient method for practical whole core calculations for prismatic VHTR design and analysis.